Quantum optical input–output relations for dispersive and lossy multilayer dielectric plates

T. Gruner and D.-G. Welsch
Friedrich-Schiller Universität Jena, Theoretisch-Physikalisches Institut
Max-Wien Platz 1, D-07743 Jena, Germany

Abstract

Using the Green function approach to the problem of quantization of the phenomenological Maxwell theory, the propagation of quantized radiation through dispersive and absorptive multilayer dielectric plates is studied. Input–output relations are derived, with special emphasis on the determination of the quantum noise generators associated with the absorption of radiation inside the dielectric matter. The input–output relations are used to express arbitrary correlation functions of the outgoing field in terms of correlation functions of the incoming field and those of the noise generators. To illustrate the theory, the effect of a single-slab plate on the mean photon-number densities in the frequency domain is discussed in more detail.

1 Introduction

It is well known that the use of instruments in optical experiments needs careful examination with regard to their action on the quantum statistics of the light under study. In particular the presence of passive instruments that may be regarded as macroscopic dielectric bodies responding linearly to radiation can be included in the theory by quantization of the phenomenological Maxwell theory for radiation in linear inhomogeneous dielectrics. The formalism was first developed for dispersionless and lossless dielectrics [1, 2, 3, 4] and successfully applied to the study of the action of various devices, such as dielectric plates and interfaces [5, 6] and optical cavities [7, 8]. When broad-band radiation, such as an ultrashort light pulse, propagates through (long-distance) dielectric devices the effects of dispersion and absorption, which are related to each other by the Kramers–Kronig relations, must necessarily be taken into account. In this context, a number of questions have been arisen, such as the question about the velocity at which a single-photon wavepacket travels in dielectric matter under the influence of normal and/or abnormal dispersion in the vicinity of an absorption line [9, 10]. Needless to say that absorption also introduces additional noise, at least the (quantum) vacuum noise.

The problem of describing the effects of dispersive and absorptive linear dielectric devices on quantized radiation has been considered in a number of papers and various quantization schemes have been proposed [11, 12, 13, 14, 15, 16, 17, 18]. As we have recently shown, quantization of the radiation field within the frame of the phenomenological Maxwell theory (with given complex permittivity in the frequency domain) can be performed using a Green-function expansion of the operator of the vector potential [17, 19]. This quantum-field-theoretical formalism, which may be regarded as a generalization of the familiar concepts of mode expansion, applies to both homogeneous and inhomogeneous dielectric matter and is consistent with both the Kramers–Kronig relations and the canonical (equal-time) field commutation relations in QED.

In the present paper we use the method in order to study the behaviour of quantized radiation in the presence of a multilayer dielectric plate and to derive input–output relations. The calculation of input–output relations is commonly based on a development of the familiar formalism of quantum noise theory (see, e.g. [20]), in which the explicit nature of the input from a heat bath, and the output into it, is taken into account. The advantage of the quantum-field-theoretical approach is that it enables one to obtain the input–output relations including their dependence on frequency through geometry and dispersive and absorptive properties of the layers, because it consistently accounts for the effects of radiation-field propagation according to the (phenomenological) quantum Maxwell equations.

It is well known that when dielectric matter in free space is considered and the imaginary part of the permittivity may be disregarded (provided that the losses

in the chosen frequency interval are sufficiently small), then the input–output relations correspond to unitary transformations between input- and output-mode operators [21, 22]. These concepts fail when the effect of absorption of radiation through the dielectric matter is taken into account. In this case the outgoing fields are not only related to the incoming fields but also to appropriately chosen noise sources [23]. Neglection of these supplementary contributions would unavoidably lead to a violation of the canonical commutation relations for the outgoing fields, and hence effects of quantum noise would left out. Knowing the input–output-relations, the quantum statistics of the outgoing fields can be obtained from the statistics of the incoming fields and internal (temperature-dependent) noise properties of the dielectric matter under study.

The input–output relations derived may be used in various quantum-optical applications, because the multilayer dielectric structure under study may serve as a model for a number of devices, such as mirrors, beam splitters, interferometers of Fabry-Pérot type, and optical fibres. In particular, multilayer dielectric mirrors may be regarded as tunnel barriers for photons [24] and can be used in order to measure barrier traversal times [9]. The apparently superluminal behaviour of photons at dielectric tunnel barriers, which has been observed in recent experiments, may be modified by the absorption in the dielectric structures [25]. These and related studies have been a subject of increasing interest in order to answer a fundamental question of quantum physics, namely, of how much time it takes a particle to tunnel through a barrier.

The paper is organized as follows. In Sec. 2 the Green function approach to the quantization of radiation in dispersive and lossy linear dielectrics is summarized. Applying this quantization scheme to radiation propagating through multilayer dielectric plates, in Sec. 3 input-output relations are derived. In Sec. 4 these relations are used to study normally ordered correlation functions of the outgoing fields. To illustrate the theory, results for the photon-number density statistics observed in the case of a single-slab dielectric plate are given. Finally, a summary and some conclusions are given in Sec. 5.

2 Quantization scheme

2.1 Green's function approach

Let us consider linearly polarized radiation propagating in x direction and allow for the the presence of a multilayer dielectric plate characterized in terms of a frequency-dependent permittivity $\epsilon(x,\omega)$ that varies in x direction and obeys, for causality reasons, the Kramers–Kronig relations. Introducing the vector potential $A(x,t)$ and using the relation

$$D(x,t) = \epsilon_0 \left[E(x,t) + \int_{-\infty}^{t} \mathrm{d}\tau \, \chi(t-\tau) E(x,\tau) \right] \tag{1}$$

($E = -\dot{A}$), the classical phenomenological Maxwell equations yield

$$\frac{\partial^2}{\partial x^2}A(x,t) - \frac{1}{c^2}\left[\ddot{A}(x,t) + \int_{-\infty}^{t} \mathrm{d}\tau\, \chi(t-\tau)\ddot{A}(x,\tau)\right] = 0, \tag{2}$$

which in the frequency domain reads as

$$\left[\frac{\partial^2}{\partial x^2} + \frac{\omega^2}{c^2}\epsilon(x,\omega)\right] A(x,\omega) = 0. \tag{3}$$

Equation (3) may be transferred to quantum theory as follows [17, 19]:

$$\left[\frac{\partial^2}{\partial x^2} + \frac{\omega^2}{c^2}\epsilon(x,\omega)\right] \hat{A}(x,\omega) = \hat{j}(x,\omega), \tag{4}$$

where the "current" operator

$$\hat{j}(x,\omega) = \frac{\omega}{c^2}\sqrt{\frac{\hbar}{\pi\epsilon_0\mathcal{A}}\,\epsilon_{\mathrm{i}}(x,\omega)}\,\hat{f}(x,\omega) \tag{5}$$

is introduced to take into account the noise owing to absorption. In Eq. (5), $\hat{f}(x,\omega)$ and $\hat{f}^\dagger(x,\omega)$ are bosonic field operators,

$$\left[\hat{f}(x,\omega), \hat{f}^\dagger(x',\omega')\right] = \delta(x-x')\,\delta(\omega-\omega'), \tag{6}$$

$$\left[\hat{f}(x,\omega), \hat{f}(x',\omega')\right] = \left[\hat{f}^\dagger(x,\omega), \hat{f}^\dagger(x',\omega')\right] = 0, \tag{7}$$

and

$$\epsilon(x,\omega) = \epsilon_{\mathrm{r}}(x,\omega) + i\,\epsilon_{\mathrm{i}}(x,\omega) \tag{8}$$

($\mathcal{A}$, normalization area in the yz plane). The solution of Eq. (4) may be given by

$$\hat{A}(x,\omega) = \int \mathrm{d}x'\, G(x,x',\omega)\hat{j}(x',\omega), \tag{9}$$

where $G(x,x',\omega)$ is the classical Green function obeying the equation

$$\left[\frac{\partial^2}{\partial x^2} + \frac{\omega^2}{c^2}\epsilon(x,\omega)\right] G(x,x',\omega) = \delta(x-x') \tag{10}$$

and tending to zero as $x \to \pm\infty$. It can be shown [17, 19], that the quantization scheme outlined above ensures that the (Schrödinger) operators of the vector potential and the electric-field strength,

$$\hat{A}(x) = \int_0^\infty \mathrm{d}\omega\, \hat{A}(x,\omega) + \mathrm{H.c.}, \tag{11}$$

$$\hat{E}(x) = i\int_0^\infty \mathrm{d}\omega\, \omega\hat{A}(x,\omega) + \mathrm{H.c.}, \tag{12}$$

satisfy the well-known canonical commutation relation

$$\left[\hat{A}(x), \hat{E}(x')\right] = -\frac{i\hbar}{\mathcal{A}\epsilon_0}\delta(x-x'). \tag{13}$$

2.2 Quantum Langevin equations

From Eqs. (11), (9), and (10) we see that the problem of determining the operator of the vector potential reduces to the calculation of the classical Green function. Before performing the calculations for multilayer dielectric plates, let us summarize some results for homogeneous dielectrics, where

$$\begin{aligned} G(x,x',\omega) &= \frac{1}{2\pi}\int_{-\infty}^{\infty} dk\, e^{ik(x-x')}\frac{c^2}{\omega^2\epsilon(\omega)-c^2k^2} \\ &= \left[2i\frac{\omega}{c}n(\omega)\right]^{-1}\exp\left[i\frac{\omega}{c}n(\omega)\,|x-x'|\right]. \end{aligned} \tag{14}$$

Here

$$n(\omega)=\sqrt{\epsilon(\omega)}=\beta(\omega)+i\,\gamma(\omega) \tag{15}$$

is the complex refractive index. Using Eqs. (9) and (14), Eq. (11) may be rewritten as

$$\hat{A}(x)=\int_0^\infty \mathrm{d}\omega\,\sqrt{\frac{\hbar}{4\pi c\omega\epsilon_0\beta(\omega)\mathcal{A}}}\,\frac{\beta(\omega)}{n(\omega)}\left[e^{i\beta(\omega)\omega x/c}\hat{a}_+(x,\omega)+e^{-i\beta(\omega)\omega x/c}\hat{a}_-(x,\omega)\right]+\mathrm{H.c.}, \tag{16}$$

where the operators

$$\hat{a}_\pm(x,\omega)=\frac{1}{i}\sqrt{2\gamma(\omega)\frac{\omega}{c}}\,e^{\mp\gamma(\omega)\omega x/c}\int_{-\infty}^{\pm x}\mathrm{d}x'\,e^{-in(\omega)\omega x'/c}\hat{f}(\pm x',\omega) \tag{17}$$

associated with the waves propagating to the right (+) and left (−) are introduced. In the limiting case when the absorption may be disregarded $[\gamma(\omega)\omega|x-x'|/c\to 0]$, Eq. (16) reduces to the familiar mode-expansion result [17, 19]. In particular, the operators $\hat{a}_\pm(x,\omega)$ and $\hat{a}^\dagger_\pm(x,\omega)$ become independent on x and satisfy the well-known commutation relations for photon destruction and creation operators, respectively.

Equation (17) implies that the operators $\hat{a}_\pm(x,\omega)$ and $\hat{a}_\pm(x',\omega)$ can be related to each other as

$$\hat{a}_\pm(x,\omega)=\hat{a}_\pm(x',\omega)e^{\mp\gamma(\omega)\omega(x-x')/c}+\int_{x'}^{x}\mathrm{d}y\,\hat{F}_\pm(y,\omega)e^{\mp\gamma(\omega)\omega(x-y)/c}, \tag{18}$$

where

$$\hat{F}_\pm(x,\omega)=\pm\frac{1}{i}\sqrt{2\gamma(\omega)\frac{\omega}{c}}\,e^{\mp i\beta(\omega)\omega x/c}\hat{f}(x,\omega). \tag{19}$$

Hence, the operators $\hat{a}_\pm(x,\omega)$ obey quantum Langevin equations in the space domain [19],

$$\frac{\partial}{\partial x}\hat{a}_\pm(x,\omega)=\mp\gamma(\omega)\frac{\omega}{c}\hat{a}_\pm(x,\omega)+\hat{F}_\pm(x,\omega), \tag{20}$$

where the operators $\hat{F}_\pm(x,\omega)$ may be regarded as Langevin noise sources,

$$\left[\hat{F}_\pm(x,\omega),\hat{F}^\dagger_\pm(x',\omega')\right]=2\gamma(\omega)\frac{\omega}{c}\delta(x-x')\delta(\omega-\omega'), \tag{21}$$

$$\left[\hat{F}_\pm(x,\omega),\hat{a}^\dagger_\pm(x',\omega')\right]=\pm\Theta\left(\pm x'\mp x\right)2\gamma(\omega)\frac{\omega}{c}\,e^{-\gamma(\omega)\omega|x'-x|/c}\delta(\omega-\omega'). \tag{22}$$

3 Input–output relations

We now turn to the problem of propagation of quantized radiation through multilayer dielectric plates. Assuming N dielectric slabs, the interfaces being parallel to the yz plane (cf. Fig. 1), the permittivity may be given by

$$\epsilon(x,\omega) = \sum_{j=1}^{N} \lambda_j(x)\epsilon_j(\omega), \tag{23}$$

where

$$\lambda_j(x) = \begin{cases} 1 & \text{if } x_{j-1} < x < x_j, \\ 0 & \text{otherwise} \end{cases} \tag{24}$$

is the characteristic function of the jth slab ($x_0 \to -\infty$, $x_N \to \infty$). In particular, for $N \geq 3$ the system represents an $(N-2)$-slab dielectric plate surrounded by dielectric matter whose permittivity on the left and right, respectively, is $\epsilon_1(\omega)$ and $\epsilon_N(\omega)$. To determine the Green function $G(x,x',\omega)$ that satisfies Eq. (10) [and vanishes at infinity], we note that $G(x,x',\omega)$ can be decomposed into two parts,

$$G(x,x',\omega) = G_0(x,x',\omega) + G_1(x,x',\omega), \tag{25}$$

where, according to Eq. (14),

$$G_0(x,x',\omega) = \sum_{j=1}^{N} \lambda_j(x)\lambda_j(x') \left[2i\frac{\omega}{c}n_j(\omega)\right]^{-1} \exp\left[i\frac{\omega}{c}n_j(\omega)\,|x-x'|\right], \tag{26}$$

and $G_1(x,x',\omega)$ is solution of the homogeneous equation

$$\left[\frac{\partial^2}{\partial x^2} + \frac{\omega^2}{c^2}\epsilon(x,\omega)\right] G_1(x,x',\omega) = 0, \tag{27}$$

which implies that

$$G_1(x,x',\omega) = \sum_{j=1}^{N} \lambda_j(x) \left[C_j^{(1)}(x',\omega)e^{in_j(\omega)\omega x/c} + C_j^{(2)}(x',\omega)e^{-in_j(\omega)\omega x/c}\right]. \tag{28}$$

Clearly, the $C_j^{(1)}(x',\omega)$ and $C_j^{(2)}(x',\omega)$ must be determined in such a way that $G(x,x',\omega)$ vanishes at infinity and is continuously differentiable at the surfaces of discontinuity. The somewhat lengthy calculations may be performed in a straightforward way. For the simplest case of a single-slab dielectric plate embedded in dielectric matter ($N=3$, cf. Fig. 1), the result is given in Appendix A. Because of the voluminous formulas, we renounce their presentation for the general case.

Combining Eqs. (9) and (25) [together with Eqs. (26) and (28)], the (Schrödinger) operator of the vector potential $\hat{A}(x)$ for the jth domain ($j=1,\ldots,N$) may be

represented as, similar to Eq. (16),

$$\hat{A}(x) = \int_0^\infty \mathrm{d}\omega \sqrt{\frac{\hbar}{4\pi c\omega\epsilon_0\beta_j(\omega)\mathcal{A}} \frac{\beta_j(\omega)}{n_j(\omega)}} \left[e^{i\beta_j(\omega)\omega x/c}\hat{a}_{j+}(x,\omega) + e^{-i\beta_j(\omega)\omega x/c}\hat{a}_{j-}(x,\omega)\right] + \mathrm{H.c.} \tag{29}$$

($x_{j-1} \le x \le x_j$), where the dependence on x of the amplitude operators $\hat{a}_{j\pm}(x,\omega)$ is governed by quantum Langevin equations of the type given in Eq. (20) together with Eqs. (19) and (21) [$\beta(\omega),\gamma(\omega) \to \beta_j(\omega),\gamma_j(\omega)$], so that $\hat{a}_{j\pm}(x,\omega)$ can be represented in the form (18), viz.

$$\begin{aligned}\hat{a}_{j\pm}(x,\omega) = {} & \hat{a}_{j\pm}(x',\omega) e^{\mp\gamma_j(\omega)\omega(x-x')/c} \\ & + \int_{x'}^{x} \mathrm{d}y\, \hat{F}_{j\pm}(y,\omega) e^{\mp\gamma_j(\omega)\omega(x-y)/c}\end{aligned} \tag{30}$$

($x_{j-1} \le x, x' \le x_j$), where

$$\hat{F}_{j\pm}(x,\omega) = \pm\frac{1}{i}\sqrt{2\gamma_j(\omega)\frac{\omega}{c}}\, e^{\mp i\beta_j(\omega)\omega x/c} \hat{f}(x,\omega). \tag{31}$$

Since the relations between the $\hat{a}_{j\pm}(x,\omega)$ and $\hat{f}(x,\omega)$ sensitively depend on the actual expression for $G(x,x',\omega)$, the commutation relations (22) [that are based on Eq. (17)] cannot be applied in general. Successive application of Eq. (30) enables one to relate the (amplitude) operators $\hat{a}_{1-}(x,\omega)$ ($-\infty \le x \le x_1$) and $\hat{a}_{N+}(x,\omega)$ ($x_{N-1} \le x \le \infty$) for the outgoing fields to the left and right, respectively, to the operators of the corresponding incoming fields, $\hat{a}_{1+}(x,\omega)$ and $\hat{a}_{N-}(x,\omega)$, and operator noise sources associated with the losses owing to absorption.

3.1 Single-slab dielectric plate

To illustrate the procedure outlined, let us first study the input–output relations for a single-slab dielectric plate of thickness l embedded in two (different) dielectrics ($N=3$, cf. Fig. 1). Substituting in Eq. (9) for $G(x,x',\omega)$ the expression (A 1) given in Appendix A and introducing the (amplitude) operators $\hat{a}_{1\pm}(x,\omega)$, $-\infty \le x \le -l/2$, and $\hat{a}_{3\pm}(x,\omega)$, $l/2 \le x \le \infty$ [Appendix B.1, Eqs. (B 1) – (B 4)], the input operators are found to satisfy the commutation relations

$$[\hat{a}_{1+}(x,\omega), \hat{a}^\dagger_{1+}(x',\omega')] = e^{-\gamma_1(\omega)|x-x'|/c}\delta(\omega-\omega'), \tag{32}$$

$$[\hat{a}_{3-}(x,\omega), \hat{a}^\dagger_{3-}(x',\omega')] = e^{-\gamma_3(\omega)|x-x'|/c}\delta(\omega-\omega'), \tag{33}$$

$$[\hat{a}_{1+}(x,\omega), \hat{a}^\dagger_{3-}(x',\omega')] = 0 \tag{34}$$

[Eqs. (B 20) – (B 22)], so that the input fields from the left and right behave like the fields in the corresponding bulk dielectrics and may be regarded as independent variables. Note that $\hat{a}_{1+}(x,\omega)$, $\hat{a}_{3-}(x,\omega)$ are commuting quantities.

Defining operators

$$\hat{g}_{\pm}^{(1)}(\omega) = [2c_{\pm}(l,\omega)]^{-\frac{1}{2}} \left[\hat{g}'_{-}(\omega) \pm \hat{g}'_{+}(\omega)\right], \tag{35}$$

where

$$\hat{g}'_{\pm}(\omega) = \frac{1}{i}\sqrt{\frac{\omega}{c}}\, e^{in_2(\omega)\omega l/(2c)} \int_{-\frac{l}{2}}^{\frac{l}{2}} \mathrm{d}x'\, e^{\mp in_2(\omega)\omega x'/c} \hat{f}(x',\omega) \tag{36}$$

and

$$c_{\pm}(l,\omega) = e^{-\gamma_2(\omega)\omega l/c} \frac{1}{\gamma_2(\omega)} \sinh\left[\gamma_2(\omega)\frac{\omega}{c} l\right] \pm e^{-\gamma_2(\omega)\omega l/c} \frac{1}{\beta_2(\omega)} \sin\left[\beta_2(\omega)\frac{\omega}{c} l\right], \tag{37}$$

and recalling Eqs. (6) and (7), we find that

$$\left[\hat{g}_{\pm}^{(1)}(\omega), (\hat{g}_{\pm}^{(1)}(\omega'))^{\dagger}\right] = \delta(\omega - \omega'), \tag{38}$$

$$\left[\hat{g}_{\pm}^{(1)}(\omega), (\hat{g}_{\mp}^{(1)}(\omega'))^{\dagger}\right] = 0. \tag{39}$$

Since

$$\left[\hat{a}_{1+}(x,\omega), (\hat{g}_{\pm}^{(1)}(\omega'))^{\dagger}\right] = 0 = \left[\hat{a}_{3-}(x',\omega), (\hat{g}_{\pm}^{(1)}(\omega'))^{\dagger}\right] \tag{40}$$

[Eq. (B 23)], the incoming-field (amplitude) operators and the operators $\hat{g}_{\pm}^{(1)}(\omega)$, $(\hat{g}_{\pm}^{(1)})^{\dagger}(\omega)$ may be regarded as being independent variables (note that $\hat{a}_{1+}$, $\hat{a}_{3-}$ and $\hat{g}_{\pm}^{(1)}$ commute). Moreover, the $\hat{g}_{\pm}^{(1)}(\omega)$ and $(\hat{g}_{\pm}^{(1)})^{\dagger}(\omega)$, respectively, which are obviously destruction and creation operators of bosonic excitations associated with the plate, play the role of the additional operator noise sources in the input–output relations

$$\begin{pmatrix} \hat{a}_{1-}(-\frac{1}{2}l,\omega) \\ \hat{a}_{3+}(\frac{1}{2}l,\omega) \end{pmatrix} = \widetilde{\mathbf{T}}^{(1)} \begin{pmatrix} \hat{a}_{1+}(-\frac{1}{2}l,\omega) \\ \hat{a}_{3-}(\frac{1}{2}l,\omega) \end{pmatrix} + \widetilde{\mathbf{A}}^{(1)} \begin{pmatrix} \hat{g}_{+}^{(1)}(\omega) \\ \hat{g}_{-}^{(1)}(\omega) \end{pmatrix} \tag{41}$$

derived in Appendix B.1 [Eq. (B 5)], the elements of the 2×2 matrices

$$\widetilde{\mathbf{T}}^{(1)} = \begin{pmatrix} T_{11}^{(1)}(\omega) & T_{12}^{(1)}(\omega) \\ T_{21}^{(1)}(\omega) & T_{22}^{(1)}(\omega) \end{pmatrix}, \tag{42}$$

and

$$\widetilde{\mathbf{A}}^{(1)} = \begin{pmatrix} A_{11}^{(1)}(\omega) & A_{12}^{(1)}(\omega) \\ A_{21}^{(1)}(\omega) & A_{22}^{(1)}(\omega) \end{pmatrix} \tag{43}$$

being given in Eqs.(B 6) – (B 13) [note the simplifications (B 14) – (B 19) when the plate is surrounded by vacuum]. In Eq. (41) the (amplitude) operators of the outgoing fields, $\hat{a}_{1-}(-l/2,\omega)$ and $\hat{a}_{3+}(l/2,\omega)$, are expressed in terms of the operators of the incoming fields, $\hat{a}_{1+}(-l/2,\omega)$ and $\hat{a}_{3-}(l/2,\omega)$, and the operator noise sources $\hat{g}_{\pm}^{(1)}(\omega)$. The characteristic transformation matrix of the plate, $\widetilde{\mathbf{T}}^{(1)}$, which for an approximately lossless dielectric plate in free space reduces to the

well-known characteristic matrix given, e.g., in [26], describes the effects of transmission and reflection of the input fields, whereas the losses inside the plate give rise to an additional matrix, $\widetilde{\mathbf{A}}^{(1)}$, which may be called characteristic absorption matrix.

It should be mentioned that the output amplitude operators $\hat{a}_{1-}(x)$, $x \leq -l/2$, and $\hat{a}_{3+}(x)$, $x \geq l/2$, can easily be obtained from Eq. (30), with $x' = -l/2$ and $x' = l/2$, respectively, and application of the input–output relations (41). The resulting representation of the outgoing fields is of course fully equivalent to the Green's function expansion primarily used. The commutation relations for the output amplitude operators are given in Appendix B.1 [Eqs. (B 24) – (B 26)]. They differ, in general, from those given in Eqs. (32) – (34) for the input operators. The differences vanish when the distances from the plate are large compared with the (classical) absorption length or when the plate is in free space.

3.2 Multilayer dielectric plates

The results given in Sec. 3.1 can be extended to an arbitrary multi-slab dielectric structure ($N \geq 3$, cf. Fig. 2) in a straightforward way (for details see Appendix B.2). In particular, the input–output relations may be given by

$$\begin{pmatrix} \hat{a}_{1-}(x_1,\omega) \\ \hat{a}_{N+}(x_{N-1},\omega) \end{pmatrix} = \widetilde{\mathbf{T}}^{(N-2)} \begin{pmatrix} \hat{a}_{1+}(x_1,\omega) \\ \hat{a}_{N-}(x_{N-1},\omega) \end{pmatrix} + \widetilde{\mathbf{A}}^{(N-2)} \begin{pmatrix} \hat{g}_{+}^{(N-2)}(\omega) \\ \hat{g}_{-}^{(N-2)}(\omega) \end{pmatrix}. \tag{44}$$

Here, $x = x_1$ and $x = x_{N-1}$, respectively, are the left and right surfaces of the multi-slab plate (note that for the single-slab plate, $N = 3$, the notations $x_1 = -l/2$ and $x_{N-1} = x_2 = l/2$ have been used). The commutation rules for the input operators $\hat{a}_{1+}(x,\omega)$, $\hat{a}_{1+}^{\dagger}(x,\omega)$ $(-\infty \leq x \leq x_1)$, $\hat{a}_{N-}(x,\omega)$, $\hat{a}_{N-}^{\dagger}(x,\omega)$ $(x_{N-1} \leq x \leq \infty)$, and the noise operators $\hat{g}_{\pm}^{(N-2)}(\omega)$ are the same as in the preceding section, i.e.,

$$[\hat{a}_{1+}(x,\omega), \hat{a}_{1+}^{\dagger}(x',\omega')] = e^{-\gamma_1(\omega)|x-x'|/c}\delta(\omega-\omega'), \tag{45}$$

$$[\hat{a}_{N-}(x,\omega), \hat{a}_{N-}^{\dagger}(x',\omega')] = e^{-\gamma_N(\omega)|x-x'|/c}\delta(\omega-\omega'), \tag{46}$$

$$[\hat{a}_{1+}(x,\omega), \hat{a}_{N-}^{\dagger}(x',\omega')] = 0, \tag{47}$$

$$\left[\hat{g}_{\pm}^{(N-2)}(\omega), (\hat{g}_{\pm}^{(N-2)}(\omega'))^{\dagger}\right] = \delta(\omega-\omega'), \tag{48}$$

$$\left[\hat{g}_{\pm}^{(N-2)}(\omega), (\hat{g}_{\mp}^{(N-2)}(\omega'))^{\dagger}\right] = 0, \tag{49}$$

$$\left[\hat{a}_{1+}(x,\omega), (\hat{g}_{\pm}^{(N-2)}(\omega'))^{\dagger}\right] = 0 = \left[\hat{a}_{N-}(x',\omega), (\hat{g}_{\pm}^{(N-2)}(\omega'))^{\dagger}\right]. \tag{50}$$

The input-output relations (44) [together with the commutation relations (45) – (50)] apply to arbitrary multi-slab dielectric equipments described in terms of a complex permittivity that spatially varies as a multi-step function and whose dependence on frequency is consistent with the Kramers–Kronig relations over the

whole frequency domain. Typical examples are fractionally transparent dielectric mirrors and combinations of them, such as resonator-like cavities bounded by dielectric walls. In particular, when the overall device is surrounded by vacuum, so that the incoming and outgoing radiation fields propagate in free space,

$$n_1(\omega) = n_N(\omega) \equiv 1, \tag{51}$$

the familiar mode expansions for the input and output (free) fields are recognized. For $j=1, N$ Eq. (29) takes the form

$$\hat{A}(x) = \int_0^\infty \mathrm{d}\omega \sqrt{\frac{\hbar}{4\pi c\omega\epsilon_0\mathcal{A}}} \left[e^{i\omega x/c}\hat{a}_{j+}(\omega) + e^{-i\omega x/c}\hat{a}_{j-}(\omega)\right] + \text{H.c.}, \tag{52}$$

where the input and output operators $\hat{a}_{1\pm}(\omega)$ $[\hat{a}^\dagger_{1\pm}(\omega)]$ and $\hat{a}_{N\pm}(\omega)$ $[\hat{a}^\dagger_{N\pm}(\omega)]$, respectively, are proper (space-independent) photon destruction [creation] operators, and

$$\begin{pmatrix} \hat{a}_{1-}(\omega) \\ \hat{a}_{N+}(\omega) \end{pmatrix} = \widetilde{\mathbf{T}}^{(N-2)} \begin{pmatrix} \hat{a}_{1+}(\omega) \\ \hat{a}_{N-}(\omega) \end{pmatrix} + \widetilde{\mathbf{A}}^{(N-2)} \begin{pmatrix} \hat{g}_+^{(N-2)}(\omega) \\ \hat{g}_-^{(N-2)}(\omega) \end{pmatrix}. \tag{53}$$

The influence of the plate on the incident light through reflection and transmission from the two sides are described by the matrix elements $T_{ik}^{(N-2)}(\omega)$, whereas the matrix elements $A_{ik}^{(N-2)}(\omega)$ arise from absorption. From Eqs. (45) – (47), the bosonic commutation relations for the input-mode operators $\hat{a}_{1+}(\omega)$, $\hat{a}_{N-}(\omega)$ are easily seen to be satisfied. Using them and recalling the commutation rules (48) – (50), the bosonic commutation relations for the output-mode operators $\hat{a}_{1-}(\omega)$, $\hat{a}_{N+}(\omega)$ can then be obtained by means of the input–output relations (53), because the relations

$$\begin{aligned} &|T_{11}^{(N-2)}|^2 + |T_{12}^{(N-2)}|^2 + |A_{11}^{(N-2)}|^2 + |A_{12}^{(N-2)}|^2 \\ &\quad = |T_{21}^{(N-2)}|^2 + |T_{22}^{(N-2)}|^2 + |A_{21}^{(N-2)}|^2 + |A_{22}^{(N-2)}|^2 = 1 \end{aligned} \tag{54}$$

and

$$\begin{aligned} &T_{11}^{(N-2)}(T_{21}^{(N-2)})^* + T_{12}^{(N-2)}(T_{22}^{(N-2)})^* \\ &\quad + A_{11}^{(N-2)}(A_{21}^{(N-2)})^* + A_{12}^{(N-2)}(A_{22}^{(N-2)})^* = 0 \end{aligned} \tag{55}$$

are valid [see Appendix B.1 and Appendix B.2]. For notational convenience, the frequency argument of the matrix elements $T_{ik}^{(N-2)}$ and $A_{ik}^{(N-2)}$ matrices are omitted. In particular, these relations reflect the fact that the sum of the probabilities for reflection, transmission, and absorption of a photon is equal to unity. If the

losses inside the plate can approximately be disregarded, $\widetilde{\mathbf{A}}^{(N-2)} \approx 0$, the well-known method of unitary transformation is recognized. In this case the relations (54) and (55) simplify to

$$|T_{11}^{(N-2)}|^2 + |T_{12}^{(N-2)}|^2 = |T_{21}^{(N-2)}|^2 + |T_{22}^{(N-2)}|^2 = 1, \tag{56}$$

$$T_{11}^{(N-2)}(T_{21}^{(N-2)})^* + T_{12}^{(N-2)}(T_{22}^{(N-2)})^* = 0, \tag{57}$$

so that $\widetilde{\mathbf{T}}^{(N-2)}$ becomes a unitary matrix. Since the photon operators of the output and input modes are uniquely related to each other through a unitary transformation, the bosonic commutation relations are automatically preserved. In general, the $\widetilde{\mathbf{T}}^{(N-2)}$ matrix is not unitary and the output-mode operators are obtained, according to Eq. (53), from both the input-mode operators and the noise operators associated with the losses. The relations (54) and (55), which are the natural generalization of the relations (56) and (57), may be regarded as necessary conditions imposed on the $\widetilde{\mathbf{T}}^{(N-2)}$ and $\widetilde{\mathbf{A}}^{(N-2)}$ matrices of an arbitrary dispersive and absorptive multi-slab dielectric device in free space. It should be emphasized that these conditions need not be postulated, but they necessarily come out of the theory, which also enables one to systematically calculate both the $\widetilde{\mathbf{T}}^{(N-2)}$ and $\widetilde{\mathbf{A}}^{(N-2)}$ matrices.

4 Radiation-field correlation functions

The input–output relations (53) can be used to obtain the quantum statistical properties of the outgoing radiation from the properties of the incoming radiation and the excitations associated with the dielectric matter. With regard to measurement, the quantum statistics of radiation is frequently described in terms of normally ordered correlation functions, such as correlation functions of the electric-field strength or the photon creation and destruction operators (see, e.g., [4, 28]). Introducing the notations $\hat{a}_1 \equiv \hat{a}_{1+}$, $\hat{a}_2 \equiv \hat{a}_{N-}$, $\hat{a}'_1 \equiv \hat{a}_{1-}$, $\hat{a}'_2 \equiv \hat{a}_{N+}$ and $\hat{g}_1 \equiv \hat{g}_+^{(N-2)}$, $\hat{g}_2 \equiv \hat{g}_-^{(N-2)}$, from Eqs. (12) and (52), the electric-field strength of the outgoing radiation in the ith channel ($i=1,2$) reads as

$$\hat{E}'_i(x) = \hat{E}'^{(+)}_i(x) + \hat{E}'^{(-)}_i(x), \tag{58}$$

$$\hat{E}'^{(+)}_i(x) = i\int_0^\infty \mathrm{d}\omega \sqrt{\frac{\hbar\omega}{4\pi c\epsilon_0\mathcal{A}}}\, e^{i\omega\eta_i x/c}\hat{a}'_i(\omega), \tag{59}$$

$$\hat{E}'^{(-)}_i(x) = \left[\hat{E}'^{(+)}_i(x)\right]^\dagger \tag{60}$$

($\eta_1 = -1$, $\eta_2 = 1$), where the output-photon operators $\hat{a}'_i(\omega)$ can be related to the input-photon operators $\hat{a}_i(\omega)$ as, according to Eq. (53),

$$\hat{a}'_i(\omega) = \sum_{k=1}^{2} \left[T_{ik}(\omega)\,\hat{a}_k(\omega) + A_{ik}(\omega)\,\hat{g}_k(\omega)\right] \tag{61}$$

$[T_{ik}(\omega) \equiv T_{ik}^{(N-2)}(\omega),\ A_{ik}(\omega) \equiv A_{ik}^{(N-2)}(\omega))$. To express the normally ordered electric-field correlation functions of the outgoing radiation,

$$C'^{(m,n)}_{\{i_\mu\}}(\{x_\mu,t_\mu\}) = \left\langle \left[\prod_{\mu=1}^{m} \hat{E}'^{(-)}_{i_\mu}(x_\mu,t_\mu)\right] \left[\prod_{\mu=m+1}^{m+n} \hat{E}'^{(+)}_{i_\mu}(x_\mu,t_\mu)\right] \right\rangle, \tag{62}$$

in terms of normally ordered correlation functions of photon creation and destruction operators, we use Eqs. (58) – (60) and recall the harmonic (exponential) time evolution of the photon destruction operators in the Heisenberg picture. We obtain

$$C'^{(m,n)}_{\{i_\mu\}}(\{x_\mu,t_\mu\}) = i^{n-m}\left(\frac{\hbar}{4\pi c\epsilon_0\mathcal{A}}\right)^{\frac{n+m}{2}}$$
$$\int_0^\infty \mathrm{d}\omega_1\,\sqrt{\omega_1}e^{i\omega_1\tau_{i_1}} \ldots \int_0^\infty \mathrm{d}\omega_{m+n}\,\sqrt{\omega_{m+n}}e^{-i\omega_{m+n}\tau_{i_{m+n}}}\,\underline{C}'^{(m,n)}_{\{i_\mu\}}(\{\omega_\mu\}) \tag{63}$$

$(\tau_{i_\mu} = t_\mu + \eta_{i_\mu} x_\mu/c)$, where

$$\underline{C}'^{(m,n)}_{\{i_\mu\}}(\{\omega_\mu\}) = \left\langle \left[\prod_{\mu=1}^{m} \hat{a}'^{\dagger}_{i_\mu}(\omega_\mu)\right] \left[\prod_{\mu=m+1}^{m+n} \hat{a}'_{i_\mu}(\omega_\mu)\right] \right\rangle, \tag{64}$$

which can be rewritten as, on using the input–output relations (61), Eq. (64),

$$\underline{C}'^{(m,n)}_{\{i_\mu\}}(\{\omega_\mu\}) = \left\langle \left\{ \prod_{\mu=1}^{m} \sum_{k_\mu=1}^{2} \left[T^*_{i_\mu k_\mu}(\omega_\mu)\,\hat{a}^\dagger_{k_\mu}(\omega_\mu) + A^*_{i_\mu k_\mu}(\omega_\mu)\,\hat{g}^\dagger_{k_\mu}(\omega_\mu)\right] \right\} \right.$$
$$\left. \times \left\{ \prod_{\mu=m+1}^{m+n} \sum_{k_\mu=1}^{2} \left[T_{i_\mu k_\mu}(\omega_\mu)\,\hat{a}_{k_\mu}(\omega_\mu) + A_{i_\mu k_\mu}(\omega_\mu)\,\hat{g}_{k_\mu}(\omega_\mu)\right] \right\} \right\rangle. \tag{65}$$

In particular, when the states of the incoming radiation and the dielectric matter are not correlated to each other, the correlation functions of the output photons, Eq. (65), can be expressed in terms of sums of products of input-photon correlation functions

$$\underline{C}^{(k,l)}_{\{i_\mu\}}(\{\omega_\mu\}) = \left\langle \left[\prod_{\mu=1}^{k} \hat{a}^\dagger_{i_\mu}(\omega_\mu)\right] \left[\prod_{\mu=l+1}^{k+l} \hat{a}_{i_\mu}(\omega_\mu)\right] \right\rangle \tag{66}$$

and correlation functions of the excitations associated with the dielectric matter,

$$\underline{\Gamma}^{(p,q)}_{\{i_\mu\}}(\{\omega_\mu\}) = \left\langle \left[\prod_{\mu=1}^{p} \hat{g}^\dagger_{i_\mu}(\omega_\mu)\right] \left[\prod_{\mu=p+1}^{p+q} \hat{g}_{i_\mu}(\omega_\mu)\right] \right\rangle, \tag{67}$$

with $k,p \le m$ and $l,q \le n$. Clearly, when the matter is prepared in an incoherent state, then the correlation functions $\underline{\Gamma}^{(p,q)}_{\{i_\mu\}}(\{\omega_\mu\})$ vanish when $p \neq q$ (explicit

expressions for the correlation functions observed when the matter is thermally excited are given in Appendix C).

To give a simple example, let us consider the photon-number density (number of photons per unit frequency) in the ith output channel ($i=1,2$),

$$N'_{\mathrm{ph}\,i}(\omega) = \left\langle \hat{a}_i'^{\dagger}(\omega)\hat{a}_i'(\omega)\right\rangle = \underline{C}'^{(1,1)}_{ii}(\omega,\omega)\,. \tag{68}$$

Using Eq. (65) and assuming that the overall state is factored, we find that

$$\begin{aligned} N'_{\mathrm{ph}\,i}(\omega) \;&=\; \sum_{k=1}^{2}\left[|T_{ik}(\omega)|^2 N_{\mathrm{ph}\,k}(\omega) + |A_{ik}(\omega)|^2 N_{\mathrm{dp}\,k}(\omega)\right] \\ &\quad + \left[T^*_{i1}(\omega)T_{i2}(\omega)\left\langle \hat{a}_1^{\dagger}(\omega)\hat{a}_2(\omega)\right\rangle + A^*_{i1}(\omega)A_{i2}(\omega)\left\langle \hat{g}_1^{\dagger}(\omega)\hat{g}_2(\omega)\right\rangle + \mathrm{c.c.}\right], \end{aligned} \tag{69}$$

where

$$N_{\mathrm{ph}\,k}(\omega) = \left\langle \hat{a}_k^{\dagger}(\omega)\hat{a}_k(\omega)\right\rangle \tag{70}$$

and

$$N_{\mathrm{dp}\,k}(\omega) = \left\langle \hat{g}_k^{\dagger}(\omega)\hat{g}_k(\omega)\right\rangle \tag{71}$$

($k=1,2$) are the number densities of the input photons and the excitations associated with the dielectric matter, respectively.

Let us first consider the case when the input field is in the vacuum state,

$$\left\langle \hat{a}_1^{\dagger}(\omega)\hat{a}_2(\omega)\right\rangle = 0, \tag{72}$$

$$N_{\mathrm{ph}\,1}(\omega) = N_{\mathrm{ph}\,2}(\omega) = 0, \tag{73}$$

and the dielectric plate is in thermal equilibrium,

$$\left\langle \hat{g}_1^{\dagger}(\omega)\hat{g}_2(\omega)\right\rangle = 0, \tag{74}$$

$$N_{\mathrm{dp}\,1}(\omega)\Delta\omega = N_{\mathrm{dp}\,2}(\omega)\Delta\omega = \frac{\mathcal{L}}{2\pi c}n_{\mathrm{th}}(\omega)\Delta\omega, \tag{75}$$

where

$$n_{\mathrm{th}}(\omega) = \frac{1}{\exp\!\left(\frac{\hbar\omega}{k_{\mathrm{B}}T}\right) - 1} \tag{76}$$

(T, temperature; k_{B}, Boltzmann constant). For the sake of convenience, in Eq. (75) we have assumed a large but finite length $\mathcal{L}$ of the quantization volume of the radiation, so that the frequency spectrum may be regarded as being discrete. Using Eqs. (72) – (75), we see that Eq. (69) reduces to

$$N'_{\mathrm{ph}\,i}(\omega) = \frac{\mathcal{L}}{2\pi c}\alpha_i(\omega)\,n_{\mathrm{th}}(\omega) \qquad (i=1,2), \tag{77}$$

where

$$\alpha_i(\omega) = \sum_{k=1}^{2}|A_{ik}(\omega)|^2 \tag{78}$$

is the (ith-side) absorption coefficient of the plate. The result (77) is in full agreement with the standard quantum theory of thermal radiation. The plate behaves like a thermal radiator which tends to a black body as the absorption becomes perfect $[\alpha_i(\omega) \to 1]$. Note that for $\mathcal{L} \to \infty$ the photon numbers per unit frequency and unit length, $N'_{\mathrm{ph\,i}}(\omega)/\mathcal{L}$, remain finite. When the plate is in thermal equilibrium and the incident light is black-body radiation,

$$N_{\mathrm{ph}\,1}(\omega)\Delta\omega = N_{\mathrm{ph}\,2}(\omega)\Delta\omega = \frac{\mathcal{L}}{2\pi c} n_{\mathrm{th}}(\omega)\Delta\omega, \tag{79}$$

the outgoing light is also expected to be black-body radiation. Indeed, combining Eqs. (71), (72), (74), using Eqs. (75), (79), and recalling the relations (54), we find that

$$N'_{\mathrm{ph}\,i}(\omega) = \frac{\mathcal{L}}{2\pi c} n_{\mathrm{th}}(\omega) \qquad (i = 1, 2). \tag{80}$$

Finally, let us consider the case when a zero-temperature dielectric plate is irradiated from one side,

$$N_{\mathrm{ph}\,1}(\omega) \geq 0, \quad N_{\mathrm{ph}\,2}(\omega) = 0, \tag{81}$$

$$N_{\mathrm{dp}\,1}(\omega) = N_{\mathrm{dp}\,2}(\omega) = 0. \tag{82}$$

From Eq. (69) we obtain, on using Eqs. (72) and (74) together with Eq. (81) and (82),

$$N'_{\mathrm{ph}\,i}(\omega) = |T_{i1}(\omega)|^2 \, N_{\mathrm{ph}\,1}(\omega) \qquad (i = 1, 2). \tag{83}$$

The mean photon-number densities in the output channels 1 and 2, respectively, are simply given by the mean input photon-number density multiplied by the reflection and transmission coefficients. In general, the overall output photon-number density is reduced below the input level owing to absorption:

$$N'_{\mathrm{ph}\,1}(\omega) + N'_{\mathrm{ph}\,2}(\omega) \leq N_{\mathrm{ph}\,1}(\omega). \tag{84}$$

In Figs. 3 and 4 the relative photon-number densities of the outgoing radiation, $\mathcal{N}_1 \equiv N'_{\mathrm{ph}\,1}(\omega) \,/\, N_{\mathrm{ph}\,1}(\omega) = |T_{11}(\omega)|^2$ and $\mathcal{N}_2 \equiv N'_{\mathrm{ph}\,2}(\omega) \,/\, N_{\mathrm{ph}\,1}(\omega) = |T_{21}(\omega)|^2$ [Eq. (83)], are shown as functions of frequency and plate thickness for a single-slab plate in free space ($\epsilon_1(\omega)=\epsilon_3(\omega)=1$). The relative photon-number density of the radiation absorbed by the plate, $\mathcal{N}_{\mathrm{a}} = [N_{\mathrm{ph}\,1}(\omega) - (N'_{\mathrm{ph}\,1}(\omega) + N'_{\mathrm{ph}\,2}(\omega))] \,/\, N_{\mathrm{ph}\,1}(\omega) = \alpha_1(\omega) = \alpha_2(\omega)$ is shown in Fig. 5. The results in Figs. 3 – 5 are given for a simple model permittivity $\epsilon(\omega) \equiv \epsilon_2(\omega)$ based on a single medium resonance,

$$\epsilon(\omega) = 1 + \frac{\omega_1^2}{\omega_0^2 - \omega^2 - i\Gamma\omega}, \tag{85}$$

which enables one to clearly distinguish the (resonance) region of frequency for which the imaginary part of the refractive index may substantially exceed the

real part from other (off-resonance) regions for which the imaginary part becomes small.

For frequencies that are small compared with the medium resonance frequency ($\omega \ll \omega_0$) the approximately real refractive index ($n(\omega) = \beta(\omega) + i\gamma(\omega) \approx \beta(\omega) \geq 1$) gives rise to a variation with the plate thickness of the transmitted and reflected numbers of photons which show the oscillating behaviour typical for a Fabry–Pérot device. In this frequency region the losses inside the plate may be disregarded. Increasing the frequency, both the real and imaginary parts of the refractive index, $\beta(\omega)$ and $\gamma(\omega)$, respectively, are increased. Increasing $\gamma(\omega)$ implies increasing probability for photon absorption in the plate. Since the number of absorbed photons increases with the thickness of the plate, the number of transmitted photons decreases with increasing plate thickness. Further, owing to the increasing absolute value of refractive index the number of photons that are reflected are increased at the expense of the number of photons that enter the plate. The two effects mentioned become more and more pronounced as ω approaches ω_0. In particular, in the vicinity of the medium resonance the number of reflected photons is substantially enhanced. The photons that enter the plate are absorbed over a short distance, so that the number of transmitted photons rapidly tends to zero when the thickness of the plate is increased. In this "surface regime" the plate behaves like a lossy mirror, the enhanced reflectivity being caused by the large absolute value of the refractive index, which results, in general, from both the real and the imaginary parts. Further increase of frequency that is associated with a decrease of the real and imaginary parts of the refractive index (region of anomalous dispersion) reduces the effects of strong reflection and absorption and the plate again becomes fractionally transparent. Needless to say, that for sufficiently high frequencies when the refractive index approaches to unity the plate becomes fully transparent. The differences in the response of the plate to the incoming radiation for the different regions of frequency are less pronounced when the value of the damping constant Γ in Eq. (85) is increased.

In practice, the permittivity is of course a much more complicated function of frequency than the model function (85), because of the multi-frequency resonance behaviour corresponding to the multi-level excitation spectrum of the medium. In Fig. 6 the real and imaginary parts of the refractive index of amorphic SiO_2 are plotted for a region of frequency including absorbing and nonabsorbing sectors [27]. To compare the results for this realistic permittivity with those for the single resonance model (85), in Fig. 7 the number of transmitted photons is shown as a function of frequency and thickness of the plate. Although Fig. 7 roughly agrees with Fig. 4, there are a number of differences in the details which obviously result from the multi-frequency resonance structure. We would like to mention that, on following the line in Appendix B.2, the characteristic transformation and absorption matrices can be calculated numerically for an arbitrary N-slab device, as we will show in a forthcoming paper.

5 Summary and conclusions

Applying the method of Green-function expansion to the quantization of radiation propagating through a multilayer dispersive and absorptive dielectric plate, we have studied the problem of calculating the proper input–output relations for the radiation field operators and presented results for the case when the radiation propagates perpendicularly to the plate. The plate is described in terms of a multistep (spatially varying) complex permittivity in the frequency domain, which is introduced phenomenologically and only required to satisfy the Kramers–Kronig relations. The advantage of the method is that it enables one to obtain input–output relations that do not only apply to regions of frequency far from the medium resonances, but they are valid, within the frame of the phenomenological linear electrodynamics, in the whole frequency domain.

In consequence of the inclusion of the losses in the theory the output-radiation field operators are found to be related to the input-radiation field operators and operator noise sources in the plate associated with the losses, in agreement with the dissipation–fluctuation theorem. Disregarding all the losses, the characteristic absorption matrix that relates the output-radiation operators to the operators noise sources vanishes and the characteristic transformation matrix that relates the output-radiation operators to the input operators reduces to a unitary matrix. The unitary transformation ensures that the bosonic commutation relations are preserved.

When the multilayer dielectric plate is embedded in an absorbing medium the input and output radiation fields can be described in terms of amplitude operators whose space dependence (owing to damping) is governed by quantum Langevin equations. Only in the limiting case when the surrounding medium can be regarded as being lossless (particularly, when the plate is embedded in free space), the amplitude operators reduce to the well-known bosonic photon operators. In this case, the characteristic transformation and absorption matrices of the plate can be shown to be related to each other through conditions that ensure preservation of the bosonic commutation relations. These conditions can be regarded as the natural generalization of the familiar unitarity conditions for lossless plates.

The input–output relations can advantageously be used in order to obtain the quantum statistics of the output radiation from that of the input radiation and the noise sources associated with the absorbing matter. With regard to measurement, we have considered normally ordered radiation field correlation functions. To illustrate the theory, we have studied the input–output relations for the (spectral) photon-number densities in more detail. Restricting attention to a single-slab dielectric plate, numerical results are presented for a single-resonance complex (model) permittivity, and the applicability of the method to realistic dielectric matter, such as SiO_2, is demonstrated.

Finally, let us briefly comment on the underlying formalism of quantization of

the phenomenological Maxwell theory for radiation in dispersive and absorptive linear media. It should be mentioned that the formalism used resembles the concepts of generalized free-field theories [29]. This type of quantum field theory has recently been applied successfully to thermo field dynamics for quantum fields [30]. The similarities between the two descriptions may provide further insight in the basic physical structure of the theory, such as the limit of vanishing absorption. In thermo field dynamics this limit corresponds to the zero-temperature limit that has been shown to be essentially non-analytical. Similar features are also found in an indeterminacy of the dispersion relations. Absorption prevents the "spatially damped photons" from exhibiting a well-determined relation between energy (frequency) and momentum (wave vector). Similarly, at finite temperature particle states achieve a continuous spectrum not only for the particle momentum but at the same time for the mass parameter (for any fixed value of the particle momentum).

Acknowledgement

We would like to thank L. Knöll for useful discussions. One of us (T.G.) is grateful to P.D. Drummond for helpful comments on the basic concepts of quantization and to P.A. Henning for the interesting discussion on thermo fields. This work was supported by the Deutsche Forschungsgemeinschaft (74021 40 223).

Appendix A Single-slab Green function

Let us consider a dielectric slab of thickness l embedded in dielectric matter that may be different on the two sides (see Fig. 1). The Green function $G(x,x',\omega)$ can be obtained from Eqs. (25), (26), and (28), with $N=3$. The coefficients $C_j^{(1)}(x',\omega)$ and $C_j^{(2)}(x',\omega)$ in Eq. (28), $j=1,2,3$, must be determined from the conditions that the Green function is continuously differentiable at the surfaces of discontinuity (that is to say, at $x=\pm l/2$) and vanishes at infinity. Note that the latter requires the coefficients $C_1^{(1)}(x',\omega)$ and $C_3^{(2)}(x',\omega)$ to be zero. Straightforward but rather lengthy calculation yields $[n_j \equiv n_j(\omega)]$

$$
\begin{aligned}
G(x,x') = &\left[2in_1\frac{\omega}{c}\right]^{-1} \Theta\!\left(-x'-\tfrac{1}{2}l\right) \Big\{\Theta\!\left(-x-\tfrac{1}{2}l\right) \Big[e^{in_1\omega|x-x'|/c} \\
&+e^{in_1\omega|(-l)/2-x'|/c} \left(r_{12}+t_{12}\vartheta e^{in_2\omega l/c} r_{23} e^{in_2\omega l/c} t_{21}\right) e^{in_1\omega|(-l)/2-x|/c}\Big] \\
&+\left[\Theta\!\left(x+\tfrac{1}{2}l\right)-\Theta\!\left(x-\tfrac{1}{2}l\right)\right] t_{12}\vartheta e^{in_1\omega|(-l)/2-x'|/c} \left(e^{in_2\omega|x-(-l)/2|/c}+r_{23}e^{in_2\omega(l+|l/2-x|/c)}\right) \\
&+\Theta\!\left(x-\tfrac{1}{2}l\right) e^{in_1\omega|(-l)/2-x'|/c} t_{12} e^{in_2\omega l/c}\vartheta t_{23} e^{in_3\omega|x-l/2|/c}\Big\} \\
&+\left[2in_2\frac{\omega}{c}\right]^{-1} \left[\Theta\left(x'+\tfrac{1}{2}l\right)-\Theta\left(x'-\tfrac{1}{2}l\right)\right]
\end{aligned}
$$

$$
\begin{aligned}
&\times \Big\{ \Theta\left(-x-\tfrac{1}{2}l\right)\vartheta\left(e^{in_2\omega|x'-(-l)/2|/c}+e^{in_2\omega|l/2-x'|/c}r_{23}e^{in_2\omega l/c}\right)t_{21}e^{in_1\omega|(-l)/2-x|/c} \\
&+\Big[\Theta\Big(x+\tfrac{1}{2}l\Big)-\Theta\Big(x-\tfrac{1}{2}l\Big)\Big]\Big[e^{in_2\omega|x-x'|/c} \\
&+\vartheta\left(e^{in_2\omega|x'-(-l)/2|/c}r_{21}e^{in_2\omega l/c}+e^{in_2\omega|l/2-x'|/c}\right)r_{23}e^{in_2\omega|l/2-x|/c} \\
&+\vartheta\left(e^{in_2\omega|x'-(-l)/2|/c}+e^{in_2\omega|l/2-x'|/c}r_{23}e^{in_2\omega l/c}\right)r_{21}e^{in_2\omega|x-(-l)/2|/c}\Big] \\
&+\Theta\left(x-\tfrac{1}{2}l\right)\vartheta\left(e^{in_2\omega|x'-(-l)/2|/c}r_{21}e^{in_2\omega l/c}+e^{in_2\omega|l/2-x'|/c}\right)t_{23}e^{in_3\omega|x-l/2|/c}\Big\} \\
&+\left[2in_3\frac{\omega}{c}\right]^{-1}\Theta\left(x'-\tfrac{1}{2}l\right)\Big\{\Theta\left(-x-\tfrac{1}{2}l\right)e^{in_3\omega|x'-l/2|/c}t_{32}\vartheta e^{in_2\omega l/c}t_{21}e^{in_1\omega|(-l)/2-x|/c} \\
&+\left[\Theta\left(x+\tfrac{1}{2}l\right)-\Theta\left(x-\tfrac{1}{2}l\right)\right]e^{in_3\omega|x'-l/2|/c}t_{32}\vartheta\Big(e^{in_2\omega|l/2-x|/c} \\
&+e^{in_2\omega l/c}r_{21}e^{in_2\omega|x-(-l)/2|/c}\Big)+\Theta\left(x-\tfrac{1}{2}l\right)\Big[e^{in_3\omega|x-x'|/c} \\
&+e^{in_3\omega|x'-l/2|/c}\left(r_{32}+t_{32}\vartheta e^{in_2\omega l/c}r_{21}e^{in_2\omega l/c}t_{23}\right)e^{in_3\omega|x-l/2|/c}\Big]\Big\}\,. \qquad \text{(A 1)}
\end{aligned}
$$

Here, the interface reflection and transmission coefficients $r_{ij} \equiv r_{ij}(\omega)$ and $t_{ij} \equiv t_{ij}(\omega)$, respectively, are defined by

$$
r_{ij}(\omega) = -r_{ji}(\omega) = \frac{n_i(\omega)-n_j(\omega)}{n_i(\omega)+n_j(\omega)}\,, \qquad \text{(A 2)}
$$

$$
t_{ij}(\omega) = \frac{2n_i(\omega)}{n_i(\omega)+n_j(\omega)}\,, \qquad \text{(A 3)}
$$

and the factor $\vartheta \equiv \vartheta(\omega)$, which arises from multiple reflections inside the slab, reads as

$$
\begin{aligned}
\vartheta(\omega) &= \sum_{j=0}^{\infty}\left[e^{in_2(\omega)\omega l/c}r_{21}(\omega)e^{in_2(\omega)\omega l/c}r_{23}(\omega)\right]^j \\
&= \left[1-e^{in_2(\omega)\omega l/c}r_{21}(\omega)e^{in_2(\omega)\omega l/c}r_{23}(\omega)\right]^{-1}. \qquad \text{(A 4)}
\end{aligned}
$$

Note that the above given form of the Green function permits of a direct physical interpretation. The terms in Eq. (A 1) simply correspond to the potential propagations of radiation from a source point x' to a point of observation, x.

Appendix B Photonic operators, noise operators, input–output relations

Appendix B.1 Single-slab dielectric plate

Substituting in Eq. (9) for $G(x,x',\omega)$ the expression (A 1) and rewriting the result (within the space intervals $-\infty \le x \le -l/2$ and $l/2 \le x \le \infty$) in the form

(29), we easily see that the amplitude operators of the incoming fields from the left and right, respectively, $\hat{a}_{1+}(x,\omega)$ and $\hat{a}_{3-}(x,\omega)$, read as

$$\hat{a}_{1+}(x,\omega) = \frac{1}{i}\sqrt{2\gamma_1(\omega)\frac{\omega}{c}}\, e^{-\gamma_1(\omega)\omega x/c} \int_{-\infty}^{x} \mathrm{d}x'\, e^{-in_1(\omega)\omega x'/c} \hat{f}(x',\omega), \tag{B 1}$$

$$\hat{a}_{3-}(x,\omega) = \frac{1}{i}\sqrt{2\gamma_3(\omega)\frac{\omega}{c}}\, e^{\gamma_3(\omega)\omega x/c} \int_{x}^{\infty} \mathrm{d}x'\, e^{in_3(\omega)\omega x'/c} \hat{f}(x',\omega) \tag{B 2}$$

$[n_j(\omega)=\beta_j(\omega)+i\gamma_j(\omega)]$, and the amplitude operators of the outgoing fields to the left and right, respectively, $\hat{a}_{1-}(x,\omega)$ and $\hat{a}_{3+}(x,\omega)$, are given by

$$\begin{aligned}
\hat{a}_{1-}(x,\omega) = {} & \frac{1}{i}\sqrt{2\gamma_1(\omega)\frac{\omega}{c}}\, e^{\gamma_1(\omega)\omega x/c} \int_{x}^{\frac{l}{2}} \mathrm{d}x'\, e^{in_1(\omega)\omega x'/c} \hat{f}(x',\omega) \\
& + e^{\gamma_1(\omega)\omega(x-l/2)/c} e^{-in_1(\omega)\omega l/c} \Big[r_{12}(\omega) + t_{12}(\omega) r_{23}(\omega) t_{21}(\omega) e^{2in_2(\omega)\omega l/c} \vartheta(\omega)\Big]\, \hat{a}_{1+}\Big(-\tfrac{1}{2}l,\omega\Big) \\
& + \sqrt{2\gamma_1(\omega)}\, e^{\gamma_1(\omega)\omega x/c}\, \frac{n_1(\omega)}{n_2(\omega)} \sqrt{\frac{\beta_2(\omega)\gamma_2(\omega)}{\beta_1(\omega)\gamma_1(\omega)}}\, \vartheta(\omega) t_{21}(\omega) e^{-in_1(\omega)\omega l/(2c)} \\
& \qquad \times \Big[\hat{g}'_-(\omega) + r_{23}(\omega) e^{in_2(\omega)\omega l/c}\, \hat{g}'_+(\omega)\Big] \\
& + e^{[\gamma_1(\omega)x - \gamma_3(\omega)l/2]\omega/c}\, \frac{n_1(\omega)}{n_3(\omega)} \sqrt{\frac{\beta_3(\omega)}{\beta_1(\omega)}} \\
& \qquad \times e^{-i[n_1(\omega)-2n_2(\omega)+n_3(\omega)]\omega l/(2c)} t_{32}(\omega) t_{21}(\omega) \vartheta(\omega)\, \hat{a}_{3-}\Big(\tfrac{1}{2}l,\omega\Big),
\end{aligned} \tag{B 3}$$

$$\begin{aligned}
\hat{a}_{3+}(x,\omega) = {} & \frac{1}{i}\sqrt{2\gamma_3(\omega)\frac{\omega}{c}}\, e^{-\gamma_3(\omega)\omega x/c} \int_{\frac{l}{2}}^{x} \mathrm{d}x'\, e^{-in_3(\omega)\omega x'/c} \hat{f}(x',\omega) \\
& + e^{-\gamma_3(\omega)\omega(x+l/2)/c} e^{-in_3(\omega)\omega l/c} \Big[r_{32}(\omega) + t_{32}(\omega) r_{21}(\omega) t_{23}(\omega) e^{2in_2(\omega)\omega l/c} \vartheta(\omega)\Big]\, \hat{a}_{3-}\Big(\tfrac{1}{2}l,\omega\Big) \\
& + \sqrt{2\gamma_3(\omega)}\, e^{-\gamma_3(\omega)\omega x/c}\, \frac{n_3(\omega)}{n_2(\omega)} \sqrt{\frac{\beta_2(\omega)\gamma_2(\omega)}{\beta_3(\omega)\gamma_3(\omega)}}\, \vartheta(\omega) t_{23}(\omega) e^{-in_3(\omega)\omega l/(2c)} \\
& \qquad \times \Big[\hat{g}'_+(\omega) + r_{21}(\omega) e^{in_2(\omega)\omega l/c}\, \hat{g}'_-(\omega)\Big] \\
& + e^{-[\gamma_1(\omega)l/2 + \gamma_3(\omega)x]\omega/c}\, \frac{n_3(\omega)}{n_1(\omega)} \sqrt{\frac{\beta_1(\omega)}{\beta_3(\omega)}} \\
& \qquad \times e^{-i[n_1(\omega)-2n_2(\omega)+n_3(\omega)]\omega l/(2c)} t_{12}(\omega) t_{23}(\omega) \vartheta(\omega)\, \hat{a}_{1+}\Big(-\tfrac{1}{2}l,\omega\Big),
\end{aligned} \tag{B 4}$$

where the operators $\hat{g}'_\pm(\omega)$ are defined in Eq. (36).

Inverting the relations (35), we may express the operators $\hat{g}'_\pm(\omega)$ in terms of the operators $\hat{g}^{(1)}_\pm(\omega)$ and rewrite Eqs. (B 3) (for $x=-l/2$) and (B 4) (for $x=l/2$) in the compact form

$$\begin{pmatrix} \hat{a}_{1-}(-\frac{1}{2}l,\omega) \\ \hat{a}_{3+}(\frac{1}{2}l,\omega) \end{pmatrix} = \widetilde{\mathbf{T}}^{(1)} \begin{pmatrix} \hat{a}_{1+}(-\frac{1}{2}l,\omega) \\ \hat{a}_{3-}(\frac{1}{2}l,\omega) \end{pmatrix} + \widetilde{\mathbf{A}}^{(1)} \begin{pmatrix} \hat{g}^{(1)}_+(\omega) \\ \hat{g}^{(1)}_-(\omega) \end{pmatrix}. \tag{B 5}$$

The elements of the characteristic transformation matrix $\widetilde{\mathbf{T}}^{(1)}$, $T_{ik}^{(1)}(\omega)$, are seen to be

$$
\begin{aligned}
T_{11}^{(1)}(\omega) = {} & e^{-i\beta_1(\omega)\omega l/c} \\
& \times \Big[r_{12}(\omega) + t_{12}(\omega) e^{2in_2\omega\omega l/c} r_{23}(\omega)\vartheta(\omega)t_{21}(\omega)\Big],
\end{aligned}
\tag{B 6}
$$

$$
\begin{aligned}
T_{12}^{(1)}(\omega) = {} & \frac{n_1(\omega)}{n_3(\omega)}\sqrt{\frac{\beta_3(\omega)}{\beta_1(\omega)}}\, e^{-i[\beta_1(\omega)+\beta_3(\omega)]\omega l/(2c)} \\
& \times t_{32}(\omega) e^{in_2(\omega)\omega l/c}\vartheta(\omega)t_{21}(\omega),
\end{aligned}
\tag{B 7}
$$

$$
\begin{aligned}
T_{21}^{(1)}(\omega) = {} & \frac{n_3(\omega)}{n_1(\omega)}\sqrt{\frac{\beta_1(\omega)}{\beta_3(\omega)}}\, e^{-i[\beta_1(\omega)+\beta_3(\omega)]\omega l/(2c)} \\
& \times t_{12}(\omega) e^{in_2(\omega)\omega l/c}\vartheta(\omega)t_{23}(\omega),
\end{aligned}
\tag{B 8}
$$

$$
\begin{aligned}
T_{22}^{(1)}(\omega) = {} & e^{-i\beta_3(\omega)\omega l/c} \\
& \times \Big[r_{32}(\omega) + t_{32}(\omega) e^{2in_2(\omega)\omega l/c} r_{21}(\omega)\vartheta(\omega)t_{23}(\omega)\Big],
\end{aligned}
\tag{B 9}
$$

and the elements of the characteristic absorption matrix $\widetilde{\mathbf{A}}^{(1)}$, $A_{ik}^{(1)}(\omega)$, read as

$$
\begin{aligned}
A_{11}^{(1)}(\omega) = {} & \sqrt{\gamma_2(\omega)\frac{\beta_2(\omega)}{\beta_1(\omega)}}\, e^{-i\beta_1(\omega)\omega l/(2c)} \\
& \times t_{12}(\omega)\vartheta(\omega)\sqrt{c_+}\Big[1 + e^{in_2(\omega)\omega l/c} r_{23}(\omega)\Big],
\end{aligned}
\tag{B 10}
$$

$$
\begin{aligned}
A_{12}^{(1)}(\omega) = {} & \sqrt{\gamma_2(\omega)\frac{\beta_2(\omega)}{\beta_1(\omega)}}\, e^{-i\beta_1(\omega)\omega l/(2c)} \\
& \times t_{12}(\omega)\vartheta(\omega)\sqrt{c_-}\Big[1 - e^{in_2(\omega)\omega l/c} r_{23}(\omega)\Big],
\end{aligned}
\tag{B 11}
$$

$$
\begin{aligned}
A_{21}^{(1)}(\omega) = {} & \sqrt{\gamma_2(\omega)\frac{\beta_2(\omega)}{\beta_3(\omega)}}\, e^{-i\beta_3(\omega)\omega l/(2c)} \\
& \times t_{32}(\omega)\vartheta(\omega)\sqrt{c_+}\Big[e^{in_2(\omega)\omega l/c} r_{21}(\omega) + 1\Big],
\end{aligned}
\tag{B 12}
$$

$$
\begin{aligned}
A_{22}^{(1)}(\omega) = {} & \sqrt{\gamma_2(\omega)\frac{\beta_2(\omega)}{\beta_3(\omega)}}\, e^{-i\beta_3(\omega)\omega l/(2c)} \\
& \times t_{32}(\omega)\vartheta(\omega)\sqrt{c_-}\Big[e^{in_2(\omega)\omega l/c} r_{21}(\omega) - 1\Big].
\end{aligned}
\tag{B 13}
$$

Note that when the plate is surrounded by vacuum,

$$
n_1(\omega) = n_3(\omega) \equiv 1,
\tag{B 14}
$$

so that

$$
\beta_1(\omega) = \beta_3(\omega) \equiv 1, \quad \gamma_1(\omega) = \gamma_3(\omega) \equiv 0,
\tag{B 15}
$$

the following relations are valid [cf. Eqs. (A 2) – (A 4)]:

$$r_{12}(\omega)=r_{32}(\omega)=\frac{1-n_2(\omega)}{1+n_2(\omega)}=-r_{21}(\omega)=-r_{23}(\omega), \tag{B 16}$$

$$t_{12}(\omega)=t_{32}(\omega)=\frac{2}{1+n_2(\omega)}\,, \tag{B 17}$$

$$t_{21}(\omega)=t_{23}(\omega)=\frac{2n_2(\omega)}{1+n_2(\omega)}\,, \tag{B 18}$$

$$\begin{aligned}\vartheta(\omega) &= \sum_{j=0}^{\infty}\left[e^{in_2(\omega)\omega l/c}r_{21}(\omega)e^{in_2(\omega)\omega l/c}r_{23}(\omega)\right]^j \\ &= \left[1-r_{21}^2(\omega)e^{2in_2(\omega)\omega l/c}\right]^{-1}.\end{aligned} \tag{B 19}$$

Using Eqs. (35) and (36) and recalling the commutation relations (6) and (7), from Eqs. (B 1) and (B 2) we derive that

$$[\hat{a}_{1+}(x,\omega),\hat{a}_{1+}^\dagger(x',\omega')]=e^{-\gamma_1(\omega)|x-x'|/c}\delta(\omega-\omega'), \tag{B 20}$$

$$[\hat{a}_{3-}(x,\omega),\hat{a}_{3-}^\dagger(x',\omega')]=e^{-\gamma_3(\omega)|x-x'|/c}\delta(\omega-\omega'), \tag{B 21}$$

$$[\hat{a}_{1+}(x,\omega),\hat{a}_{3-}^\dagger(x',\omega')]=0, \tag{B 22}$$

$$\left[\hat{a}_{1+}(x,\omega),(\hat{g}_\pm^{(1)}(\omega'))^\dagger\right]=0=\left[\hat{a}_{3-}(x',\omega),(\hat{g}_\pm^{(1)}(\omega'))^\dagger\right]. \tag{B 23}$$

The commutation relations for the output amplitude operators $\hat{a}_{1-}(x,\omega)$, $\hat{a}_{3+}(x,\omega)$ and $\hat{a}_{1-}^\dagger(x,\omega)$, $\hat{a}_{3+}^\dagger(x,\omega)$ can be derived in a similar way or, more easily, using Eqs. (30) and (31) and applying the input–output relations (B 5) (together with the corresponding commutation relations). Straightforward calculation yields

$$\begin{aligned}&[\hat{a}_{1-}(x,\omega),\hat{a}_{1-}^\dagger(x',\omega')]=\delta(\omega-\omega')\Big\{e^{-\gamma_1(\omega)\omega|x-x'|/c} \\ &\quad+e^{-\gamma_1(\omega)\omega(|x-(-l/2)|/c+|x'-(-l/2)|/c)}\Big[|T_{11}^{(1)}(\omega)|^2+|T_{12}^{(1)}(\omega)|^2+|A_{11}^{(1)}(\omega)|^2+|A_{12}^{(1)}(\omega)|^2-1 \\ &\quad+i\frac{\gamma_1(\omega)}{\beta_1(\omega)}\left[T_{11}^{(1)}(\omega)(e^{i\beta_1(\omega)\omega l}-e^{-2i\beta_1(\omega)\omega x'})-(T_{11}^{(1)}(\omega))^*(e^{-i\beta_1(\omega)\omega l}-e^{2i\beta_1(\omega)\omega x})\right]\Big]\Big\},\end{aligned} \tag{B 24}$$

$$\begin{aligned}&[\hat{a}_{3+}(x,\omega),\hat{a}_{3+}^\dagger(x',\omega')]=\delta(\omega-\omega')\Big\{e^{-\gamma_3(\omega)\omega|x-x'|/c} \\ &\quad+e^{-\gamma_3(\omega)\omega(|x-l/2|/c+|x'-l/2|/c)}\Big[|T_{21}^{(1)}(\omega)|^2+|T_{22}^{(1)}(\omega)|^2+|A_{21}^{(1)}(\omega)|^2+|A_{22}^{(1)}(\omega)|^2-1 \\ &\quad+i\frac{\gamma_3(\omega)}{\beta_3(\omega)}\left[T_{22}^{(1)}(\omega)(e^{i\beta_3(\omega)\omega l}-e^{2i\beta_3(\omega)\omega x'})-(T_{22}^{(1)}(\omega))^*(e^{-i\beta_3(\omega)\omega l}-e^{-2i\beta_3(\omega)\omega x})\right]\Big]\Big\},\end{aligned} \tag{B 25}$$

$$
\begin{aligned}
&[\hat{a}_{3+}(x,\omega),\hat{a}^\dagger_{1-}(x',\omega')] = \delta(\omega-\omega')\Big\{ e^{-\gamma_1(\omega)\omega|x'-(-l/2)|/c-\gamma_3(\omega)\omega|x-l/2|/c)} \\
&\quad\times\Big[(T^{(1)}_{11}(\omega))^* T^{(1)}_{21}(\omega) + (T^{(1)}_{12}(\omega))^* T^{(1)}_{22}(\omega) + (A^{(1)}_{11}(\omega))^* A^{(1)}_{21}(\omega) + (A^{(1)}_{12}(\omega))^* A^{(1)}_{22}(\omega) \\
&\qquad + i\, T^{(1)}_{21}(\omega)\,\frac{\gamma_1(\omega)}{\beta_1(\omega)}\left(e^{i\beta_1(\omega)\omega l/c} - e^{-2i\beta_1(\omega)\omega x'/c}\right) \\
&\qquad\qquad + i\,(T^{(1)}_{12}(\omega))^*\frac{\gamma_3(\omega)}{\beta_3(\omega)}\left(e^{-2i\beta_3(\omega)\omega x/c} - e^{-i\beta_3(\omega)\omega l/c}\right)\Big]\Big\}.
\end{aligned}
\tag{B 26}
$$

Needless to say that $\hat{a}_{1-}(x,\omega)$ and $\hat{a}_{3+}(x,\omega)$ are commuting quantities. Using Eqs. (B 6) – (B 13) and assuming that the plate is embedded in non-absorbing media ($\gamma_1(\omega)=\gamma_3(\omega)=0$), the following relations are easily proved correct:

$$
\begin{aligned}
&|T^{(1)}_{11}(\omega)|^2 + |T^{(1)}_{12}(\omega)|^2 + |A^{(1)}_{11}(\omega)|^2 + |A^{(1)}_{12}(\omega)|^2 \\
&\quad = |T^{(1)}_{21}(\omega)|^2 + |T^{(1)}_{22}(\omega)|^2 + |A^{(1)}_{21}(\omega)|^2 + |A^{(1)}_{22}(\omega)|^2 = 1,
\end{aligned}
\tag{B 27}
$$

$$
\begin{aligned}
&T^{(1)}_{11}(\omega)(T^{(1)}_{21}(\omega))^* + T^{(1)}_{12}(\omega)(T^{(1)}_{22}(\omega))^* \\
&\quad + A^{(1)}_{11}(\omega)(A^{(1)}_{21}(\omega))^* + A^{(1)}_{12}(\omega)(A^{(1)}_{22}(\omega))^* = 0.
\end{aligned}
\tag{B 28}
$$

In this case, both the input-field commutation relations (B 20) – (B 22) and the output-field commutation relations (B 24) – (B 26) obviously reduce to the familiar bosonic commutation relations for photon destruction and creation operators.

Appendix B.2 Multi-slab dielectric plates

Starting from the results derived in Appendix B.1 for a single-slab dielectric plate ($N=3$), the results for an arbitrary dielectric plate ($N\geq 3$, cf. Fig. 2) can be obtained step by step, without explicitly calculating the multi-slab Green function. For this purpose we show that when Eqs. (44) – (50) are valid for $N-1$, then they are also valid for N. Using Eq. (44), with $N-1$ in place of N, and expressing the operators $\hat{a}_{N-1\,\pm}(x_{N-2},\omega)$ in terms of the operators $\hat{a}_{1\pm}(x_1,\omega)$, we find that

$$
\begin{pmatrix} \hat{a}_{N-1\,+}(x_{N-2},\omega) \\ \hat{a}_{N-1\,-}(x_{N-2},\omega) \end{pmatrix} = \widetilde{\mathbf{P}} \begin{pmatrix} \hat{a}_{1-}(x_1,\omega) \\ \hat{a}_{1+}(x_1,\omega) \end{pmatrix} + \widetilde{\mathbf{Q}} \begin{pmatrix} \hat{g}^{(N-3)}_{+}(\omega) \\ \hat{g}^{(N-3)}_{-}(\omega) \end{pmatrix},
\tag{B 29}
$$

where the matrices $\widetilde{\mathbf{P}}\equiv\widetilde{\mathbf{P}}^{(N-3)}$ and $\widetilde{\mathbf{Q}}\equiv\widetilde{\mathbf{Q}}^{(N-3)}$ are given by

$$
\widetilde{\mathbf{P}} \;=\; \left(T^{(N-3)}_{12}\right)^{-2} \begin{pmatrix} T^{(N-3)}_{22} & T^{(N-3)}_{21}T^{(N-3)}_{12} - T^{(N-3)}_{22}T^{(N-3)}_{11} \\ 1 & -T^{(N-3)}_{11} \end{pmatrix},
\tag{B 30}
$$

$$\widetilde{\mathbf{Q}} = \left(T_{12}^{(N-3)}\right)^{-2}$$
$$\times \begin{pmatrix} A_{21}^{(N-3)}T_{12}^{(N-3)} - A_{11}^{(N-3)}T_{22}^{(N-3)} & A_{22}^{(N-3)}T_{12}^{(N-3)} - A_{12}^{(N-3)}T_{22}^{(N-3)} \\ -A_{11}^{(N-3)} & -A_{12}^{(N-3)} \end{pmatrix} \quad \text{(B 31)}$$

The desired $(N-2)$-slab plate can be obtained by supplement to the $(N-3)$-slab plate of the $(N-1)$th slab (cf. Fig. 2). Applying Eq. (30) to $\hat{a}_{N-1\,\pm}(x,\omega)$ $(x_{N-2}\leq x\leq x_{N-1})$ yields

$$\hat{a}_{N-1\,\pm}(x_{N-1},\omega) = \hat{a}_{N-1\,\pm}(x_{N-2},\omega)e^{\mp\gamma_{N-1}(\omega)\,\omega l_{N-1}/c} + \hat{d}'_{N-1\,\pm}(\omega), \quad \text{(B 32)}$$

where $l_{N-1}=x_{N-1}-x_{N-2}$, and

$$\hat{d}'_{N-1\,\pm}(\omega) = \int_{x_{N-2}}^{x_{N-1}} \mathrm{d}y\, \hat{F}_{N-1\,\pm}(y,\omega)e^{\mp\gamma_{N-1}(\omega)\,\omega(x_{N-1}-y)/c}, \quad \text{(B 33)}$$

with $\hat{F}_{N-1\,\pm}(y,\omega)$ according to Eq. (31). Recalling the commutation relations (21), the operators $\hat{d}'_{N-1\,\pm}$ are found to satisfy the commutation relations

$$\left[\hat{d}'_{N-1\,\pm}(\omega), \hat{d}'^{\dagger}_{N-1\,\pm}(\omega')\right] = 2\delta(\omega-\omega')e^{\mp\gamma_{N-1}(\omega)\,\omega l_{N-1}/c}\sinh\!\left[\gamma_{N-1}(\omega)\frac{\omega}{c}l_{N-1}\right], \quad \text{(B 34)}$$

$$\left[\hat{d}'_{N-1\,\pm}(\omega), \hat{d}'^{\dagger}_{N-1\,\mp}(\omega')\right] = -2\delta(\omega-\omega')\frac{\gamma_{N-1}(\omega)}{\beta_{N-1}(\omega)}$$
$$\times\, e^{\mp i\beta_{N-1}(\omega)\,\omega(x_{N-2}+x_{N-1})/c}\sin\!\left[\beta_{N-1}(\omega)\frac{\omega}{c}l_{N-1}\right]. \quad \text{(B 35)}$$

By means of linear combination of the operators $\hat{d}'_{N-1\,\pm}$, bosonic operators $\hat{d}_{N-1\,\pm}$ can be introduced as

$$\begin{pmatrix} \hat{d}_{N-1\,+}(\omega) \\ \hat{d}_{N-1\,-}(\omega) \end{pmatrix} = \widetilde{\mathbf{D}} \begin{pmatrix} \hat{d}'_{N-1\,+}(\omega) \\ \hat{d}'_{N-1\,-}(\omega) \end{pmatrix}, \quad \text{(B 36)}$$

$$\left[\hat{d}_{N-1\,\pm}(\omega), \hat{d}^{\dagger}_{N-1\,\pm}(\omega')\right] = \delta(\omega-\omega'), \quad \text{(B 37)}$$
$$\left[\hat{d}_{N-1\,\pm}(\omega), \hat{d}^{\dagger}_{N-1\,\mp}(\omega')\right] = 0. \quad \text{(B 38)}$$

In Eq. (B 36), the matrix $\widetilde{\mathbf{D}}$ reads as

$$D_{11} = \left\{2\left[\alpha_+ + \left(\frac{\alpha_+}{\alpha_-}\right)^{\frac{1}{2}}|\alpha_0|\right]\right\}^{-\frac{1}{2}}, \quad \text{(B 39)}$$

$$D_{21} = -\left\{2\left[\alpha_+ - \left(\frac{\alpha_+}{\alpha_-}\right)^{\frac{1}{2}}|\alpha_0|\right]\right\}^{-\frac{1}{2}}, \quad \text{(B 40)}$$

$$D_{12} = \exp\left[i\arg[\alpha_0]\right] \left\{ 2\left[\alpha_- + \left(\frac{\alpha_-}{\alpha_+}\right)^{\frac{1}{2}} |\alpha_0| \right] \right\}^{-\frac{1}{2}}, \tag{B 41}$$

$$D_{22} = \exp\left[i\arg[\alpha_0]\right] \left\{ 2\left[\alpha_- - \left(\frac{\alpha_-}{\alpha_+}\right)^{\frac{1}{2}} |\alpha_0| \right] \right\}^{-\frac{1}{2}}, \tag{B 42}$$

where

$$\alpha_\pm = 2e^{\mp\gamma_{N-1}(\omega)\,\omega l_{N-1}/c} \sinh\left[\gamma_{N-1}(\omega)\frac{\omega}{c} l_{N-1}\right], \tag{B 43}$$

$$\alpha_0 = -2\frac{\gamma_{N-1}(\omega)}{\beta_{N-1}(\omega)} e^{-i\beta_{N-1}(\omega)\,\omega(x_{N-2}+x_{N-1})/c} \sin\left[\beta_{N-1}(\omega)\frac{\omega}{c} l_{N-1}\right]. \tag{B 44}$$

Combining Eqs. (B 32) and (B 36) we may write

$$\begin{pmatrix} \hat{a}_{N-1+}(x_{N-1},\omega) \\ \hat{a}_{N-1-}(x_{N-1},\omega) \end{pmatrix} = \widetilde{\mathbf{R}} \begin{pmatrix} \hat{a}_{N-1+}(x_{N-2},\omega) \\ \hat{a}_{N-1-}(x_{N-2},\omega) \end{pmatrix} + \widetilde{\mathbf{D}}^{-1} \begin{pmatrix} \hat{d}_{N-1+}(\omega) \\ \hat{d}_{N-1-}(\omega) \end{pmatrix}, \tag{B 45}$$

where $R_{ii'} = R_{ii}\,\delta_{ii'}$, with

$$R_{11} = R_{22}^{-1} = \exp\left[-\gamma_{N-1}(\omega)\frac{\omega}{c} l_{N-1}\right]. \tag{B 46}$$

We now relate the operators $\hat{a}_{N\pm}(x_{N-1},\omega)$ and $\hat{a}_{N-1\pm}(x_{N-1},\omega)$ to each other, applying Eqs. (29) and (30) and recalling that $\hat{A}(x)$ is continuously differentiable at x_{N-1}. Straightforward calculation yields

$$\begin{pmatrix} \hat{a}_{N+}(x_{N-1},\omega) \\ \hat{a}_{N-}(x_{N-1},\omega) \end{pmatrix} = \widetilde{\mathbf{S}} \begin{pmatrix} \hat{a}_{N-1+}(x_{N-1},\omega) \\ \hat{a}_{N-1-}(x_{N-1},\omega) \end{pmatrix}, \tag{B 47}$$

where the elements of the matrix $\widetilde{\mathbf{S}}$ read as

$$S_{11} = \sqrt{\frac{\beta_{N-1}(\omega)}{\beta_N(\omega)}} \frac{n_N(\omega) + n_{N-1}(\omega)}{2n_{N-1}(\omega)}\, e^{-i[\beta_N(\omega)-\beta_{N-1}(\omega)]\omega x_{N-1}/c}, \tag{B 48}$$

$$S_{12} = \sqrt{\frac{\beta_{N-1}(\omega)}{\beta_N(\omega)}} \frac{n_N(\omega) - n_{N-1}(\omega)}{2n_{N-1}(\omega)}\, e^{-i[\beta_N(\omega)+\beta_{N-1}(\omega)]\omega x_{N-1}/c}, \tag{B 49}$$

$$S_{21} = \sqrt{\frac{\beta_{N-1}(\omega)}{\beta_N(\omega)}} \frac{n_N(\omega) - n_{N-1}(\omega)}{2n_{N-1}(\omega)}\, e^{i[\beta_N(\omega)+\beta_{N-1}(\omega)]\omega x_{N-1}/c}, \tag{B 50}$$

$$S_{22} = \sqrt{\frac{\beta_{N-1}(\omega)}{\beta_N(\omega)}} \frac{n_N(\omega) + n_{N-1}(\omega)}{2n_{N-1}(\omega)}\, e^{i[\beta_N(\omega)-\beta_{N-1}(\omega)]\omega x_{N-1}/c}. \tag{B 51}$$

Combining Eqs. (B 29), (B 45), and (B 47), we obtain

$$\begin{pmatrix} \hat{a}_{N+}(x_{N-1},\omega) \\ \hat{a}_{N-}(x_{N-1},\omega) \end{pmatrix} = \widetilde{\mathbf{S}}\widetilde{\mathbf{R}}\widetilde{\mathbf{P}} \begin{pmatrix} \hat{a}_{1-}(x_1,\omega) \\ \hat{a}_{1+}(x_1,\omega) \end{pmatrix}$$
$$+ \widetilde{\mathbf{S}}\widetilde{\mathbf{R}}\widetilde{\mathbf{Q}} \begin{pmatrix} \hat{g}_+^{(N-3)}(\omega) \\ \hat{g}_-^{(N-3)}(\omega) \end{pmatrix} + \widetilde{\mathbf{S}}\widetilde{\mathbf{D}}^{-1} \begin{pmatrix} \hat{d}_{N-1+}(\omega) \\ \hat{d}_{N-1-}(\omega) \end{pmatrix}, \tag{B 52}$$

from which we deduce that

$$\begin{pmatrix} \hat{a}_{1-}(x_1,\omega) \\ \hat{a}_{N+}(x_{N-1},\omega) \end{pmatrix} = \widetilde{\mathbf{T}}^{(N-2)} \begin{pmatrix} \hat{a}_{1+}(x_1,\omega) \\ \hat{a}_{N-}(x_{N-1},\omega) \end{pmatrix}$$
$$+\widetilde{\mathbf{A}}' \begin{pmatrix} \hat{g}_{+}^{(N-3)}(\omega) \\ \hat{g}_{-}^{(N-3)}(\omega) \end{pmatrix} + \widetilde{\mathbf{A}}'' \begin{pmatrix} \hat{d}_{N-1\,+}(\omega) \\ \hat{d}_{N-1\,-}(\omega) \end{pmatrix}, \qquad \text{(B 53)}$$

where the matrices read as

$$\widetilde{\mathbf{T}}^{(N-2)} = (SRP)_{21}^{-2} \begin{pmatrix} -(SRP)_{22} & 1 \\ (SRP)_{12}(SRP)_{21}-(SRP)_{11}(SRP)_{22} & (SRP)_{11} \end{pmatrix}, \qquad \text{(B 54)}$$

$$\widetilde{\mathbf{A}}' = (SRP)_{21}^{-2}$$
$$\times \begin{pmatrix} -(SRQ)_{21} & -(SRQ)_{22} \\ (SRQ)_{11}(SRP)_{21}-(SRQ)_{21}(SRP)_{11} & (SRQ)_{12}(SRP)_{21}-(SRQ)_{22}(SRP)_{11} \end{pmatrix}, \qquad \text{(B 55)}$$

$$\widetilde{\mathbf{A}}'' = (SRP)_{21}^{-2}$$
$$\times \begin{pmatrix} -(SD^{-1})_{21} & -(SD^{-1})_{22} \\ (SD^{-1})_{11}(SRP)_{21}-(SD^{-1})_{21}(SRP)_{11} & (SD^{-1})_{12}(SRP)_{21}-(SD^{-1})_{22}(SRP)_{11} \end{pmatrix}. \qquad \text{(B 56)}$$

Note that $\hat{g}_{\pm}^{(N-3)}(\omega)$ and $\hat{d}_{N-1\,\pm}^{\dagger}(\omega)$ are commuting quantities, because they refer to different space intervals [cf. the commutation relations (6) or (21)].

Finally, we introduce bosonic operators $\hat{g}_{\pm}^{(N-2)}(\omega)$ as linear combinations of the operators $\hat{g}_{\pm}^{(N-3)}(\omega)$ and $\hat{d}_{N-1\,\pm}(\omega)$:

$$\begin{pmatrix} \hat{g}_{+}^{(N-2)}(\omega) \\ \hat{g}_{-}^{(N-2)}(\omega) \end{pmatrix} = \widetilde{\mathbf{U}} \left[\widetilde{\mathbf{A}}' \begin{pmatrix} \hat{g}_{+}^{(N-3)}(\omega) \\ \hat{g}_{-}^{(N-3)}(\omega) \end{pmatrix} + \widetilde{\mathbf{A}}'' \begin{pmatrix} \hat{d}_{N-1\,+}(\omega) \\ \hat{d}_{N-1\,-}(\omega) \end{pmatrix} \right] \qquad \text{(B 57)}$$

$$\left[\hat{g}_{\pm}^{(N-2)}(\omega), (\hat{g}_{\pm}^{(N-2)}(\omega'))^{\dagger}\right] = \delta(\omega-\omega'), \qquad \text{(B 58)}$$
$$\left[\hat{g}_{\pm}^{(N-2)}(\omega), (\hat{g}_{\mp}^{(N-2)}(\omega'))^{\dagger}\right] = 0. \qquad \text{(B 59)}$$

The elements of the matrix $\widetilde{\mathbf{U}}$ are given by

$$U_{11} = \left\{ 2 \left[\mu_{+} + \left(\frac{\mu_{+}}{\mu_{-}} \right)^{\frac{1}{2}} |\mu_0| \right] \right\}^{-\frac{1}{2}}, \qquad \text{(B 60)}$$

$$U_{21} = -\left\{2\left[\mu_+ - \left(\frac{\mu_+}{\mu_-}\right)^{\frac{1}{2}} |\mu_0|\right]\right\}^{-\frac{1}{2}}, \qquad \text{(B 61)}$$

$$U_{12} = \exp\left[i\arg[\mu_0]\right]\left\{2\left[\mu_- + \left(\frac{\mu_-}{\mu_+}\right)^{\frac{1}{2}} |\mu_0|\right]\right\}^{-\frac{1}{2}}, \qquad \text{(B 62)}$$

$$U_{22} = \exp\left[i\arg[\mu_0]\right]\left\{2\left[\mu_- - \left(\frac{\mu_-}{\mu_+}\right)^{\frac{1}{2}} |\mu_0|\right]\right\}^{-\frac{1}{2}}, \qquad \text{(B 63)}$$

where

$$\mu_+ = |A'_{11}|^2 + |A'_{12}|^2 + |A''_{11}|^2 + |A''_{12}|^2, \qquad \text{(B 64)}$$

$$\mu_- = |A'_{21}|^2 + |A'_{22}|^2 + |A''_{21}|^2 + |A''_{22}|^2, \qquad \text{(B 65)}$$

$$\mu_0 = A'_{11}A'^*_{21} + A'_{12}A'^*_{22} + A''_{11}A''^*_{21} + A''_{12}A''^*_{22}. \qquad \text{(B 66)}$$

Identifying the the inverse of $\widetilde{\mathbf{U}}$ with $\widetilde{\mathbf{A}}^{(N-2)}$,

$$\widetilde{\mathbf{A}}^{(N-2)} = \widetilde{\mathbf{U}}^{-1}_{,} \qquad \text{(B 67)}$$

Eq. (B 53) [together with Eq. (B 57)] is the desired result (44). From the structure of the Green function [cf. Eqs. (25) – (28)] it is clear that the input operators $\hat{a}_{1+}(x,\omega)$ and $\hat{a}_{N-}(x,\omega)$, respectively, can always be written in the form given in Eqs. (B 1) and (B 2) [with arbitrary N ($N\geq 3$) in place of $N=3$]. With regard to the basic-field operators $\hat{f}(x,\omega)$, both the input operators and the noise operators $\hat{g}^{(N-2)}_{\pm}(\omega)$ refer to different space intervals. Hence, all the commutation relations (45) – (50) are satisfied for arbitrary N ($N \geq 3$), which implies that the commutation relations (B 24) – (B 26) remain also valid when $\hat{a}_{N+}(x,\omega), \hat{a}^\dagger_{N+}(x',\omega)$ and $\widetilde{\mathbf{T}}^{(N-2)}, \widetilde{\mathbf{A}}^{(N-2)}$ are substituted for $\hat{a}_{3+}(x,\omega), \hat{a}^\dagger_{3+}(x',\omega)$ and $\widetilde{\mathbf{T}}^{(1)}, \widetilde{\mathbf{A}}^{(1)}$, respectively. We finally mention that in a way similar to that outlined above for the input–output relations the extension of the relations (B 27) and (B 28) to arbitrary N ($N\geq 3$) may be proved correct.

Appendix C Output correlation functions

When the dielectric plate is in thermal equilibrium the density operator of the matter excitations may be given by

$$\hat{\varrho}_{\rm dp} = \exp\left\{-\sum_{i=1}^{2}\int_0^\infty {\rm d}\omega\, \ln[1+n_{\rm th}(\omega)]\,\frac{\hbar\omega}{k_{\rm B}T}\,\hat{g}^\dagger_i(\omega)\hat{g}_i(\omega)\right\}, \qquad \text{(C 1)}$$

with $n_{\rm th}(\omega)$ from Eq. (76). Note that this density operator of course corresponds to the thermal-equilibrium state of the basic field $\hat{f}(x,\omega)$ inside the plate. The

correlation functions (67) are then calculated to be

$$\underline{\Gamma}^{(p,q)}_{\{i_\mu\}}(\{\omega_\mu\}) = \delta_{pq} \prod_{\zeta=1}^{p} \delta_{i_\zeta i_{\zeta+p}} n_{\rm th}(\omega_\zeta)\, \delta(\omega_\zeta - \omega_{\zeta+p}), \tag{C 2}$$

where the set of indices ζ denotes a permutation of the set of indices μ, so that $\omega_{\zeta-1} < \omega_\zeta$ for $2 \le \zeta \le p$ or $p+2 \le \zeta \le p+q$ (note that $\underline{\Gamma}^{(p,q)}_{\{i_\mu\}}(\{\omega_\mu\})$ vanishes if for any ζ with $p \ge \zeta \ge 2$ the relation $\omega_{\zeta-1} = \omega_\zeta$ is fulfilled).

We now appropriately label the terms that (after disentangling) occur on the right-hand side of Eq. (65). For this purpose we introduce the set $S^{(m,n)}$ of arrangements of the $m+n$ indices ζ (disposed in ascending order) by assigning them to two classes ($K=1,2$) and four (possibly empty) groups ($j=1,2,3,4$). The class indices $K=1$ and $K=2$ refer to the creation and destruction operators, respectively, and the group indices $j=1,2,3,4$ are used to distinguish between the four excitations to be considered. For $K=1\,(2)$ the indices refer for $j=1$ to $\hat{a}_1^\dagger$ $(\hat{a}_1)$, for $j=2$ to $\hat{a}_2^\dagger$ $(\hat{a}_2)$, for $j=3$ to $\hat{g}_1^\dagger$ $(\hat{g}_1)$, and for $j=4$ to $\hat{g}_2^\dagger$ $(\hat{g}_2)$. The λ_j^K indices of the Kth class and jth group are denoted by $\zeta_j^K(i)$, $i=1,\ldots,\lambda_j^K$. From Eq. (65) we then find that

$$\begin{aligned}
\underline{C}'^{(m,n)}_{\{i_\mu\}}(\{\omega_\mu\}) = \sum_{S^{(m,n)}} & \underline{C}^{(\lambda_1^1,\lambda_1^2;\lambda_2^1,\lambda_2^2)}_{\{i_{\zeta_1};i_{\zeta_2}\}}(\{\omega_{\zeta_1};\omega_{\zeta_2}\}) \underline{\Gamma}^{(\lambda_3^1,\lambda_3^2)}_{\{i_{\zeta_3}\}}(\{\omega_{\zeta_3}\})\, \underline{\Gamma}^{(\lambda_4^1,\lambda_4^2)}_{\{i_{\zeta_4}\}}(\{\omega_{\zeta_4}\}) \\
\times & \prod_{\alpha=1}^{\lambda_1^1} \prod_{\beta=1}^{\lambda_2^1} \prod_{\gamma=1}^{\lambda_1^2} \prod_{\eta=1}^{\lambda_2^2} T^*_{i_{\zeta_1^1(\alpha)}1}(\omega_{\zeta_1^1(\alpha)})\, T^*_{i_{\zeta_2^1(\beta)}2}(\omega_{\zeta_2^1(\beta)})\, T_{i_{\zeta_1^2(\gamma)}1}(\omega_{\zeta_1^2(\gamma)})\, T_{i_{\zeta_2^2(\eta)}2}(\omega_{\zeta_2^2(\eta)}) \\
\times & \prod_{\phi=1}^{\lambda_3^1} \left| A_{i_{\zeta_3^1(\phi)}1}(\omega_{\zeta_3^1(\phi)}) \right|^2 \prod_{\chi=1}^{\lambda_4^1} \left| A_{i_{\zeta_4^1(\chi)}2}(\omega_{\zeta_4^1(\chi)}) \right|^2,
\end{aligned} \tag{C 3}$$

where

$$\begin{aligned}
& \underline{C}^{(\lambda_1^1,\lambda_1^2;\lambda_2^1,\lambda_2^2)}_{\{i_{\zeta_1};i_{\zeta_2}\}}(\{\omega_{\zeta_1};\omega_{\zeta_2}\}) \\
& \quad = \left\langle \left[\prod_{\alpha=1}^{\lambda_1^1} \hat{a}_1^\dagger(\omega_{\zeta_1^1(\alpha)}) \right] \left[\prod_{\beta=1}^{\lambda_2^1} \hat{a}_2^\dagger(\omega_{\zeta_2^1(\beta)}) \right] \left[\prod_{\gamma=1}^{\lambda_1^2} \hat{a}_1(\omega_{\zeta_1^2(\gamma)}) \right] \left[\prod_{\eta=1}^{\lambda_2^2} \hat{a}_2(\omega_{\zeta_2^2(\eta)}) \right] \right\rangle
\end{aligned} \tag{C 4}$$

(the notation ζ_j is used to indicate sets of indices, without distinguishing between the two classes).

References

[1] L. Knöll, W. Vogel, and D.-G. Welsch, Phys. Rev. A **36**, 3803 (1987).

[2] R.J. Glauber and M. Lewenstein, Phys. Rev. A **43**, 467 (1991).

[3] H. Khosravi and R. Loudon, Proc. R. Soc. Lond. Ser. A **433**, 337 (1991); *ibid.* **436**, 373 (1992).

[4] W. Vogel and D.-G. Welsch, *Lectures on Quantum Optics* (Akademie Verlag, Berlin, 1994).

[5] L. Knöll, W. Vogel, and D.–G. Welsch, Phys. Rev. A **42**, 503 (1990); J. Opt. Soc. Am. B **3**, 1315 (1986).

[6] L. Allen and S. Stenholm, Opt. Commun. **93**, 253 (1992).

[7] L. Knöll, W. Vogel, and D.-G. Welsch, Phys. Rev. A **43**, 543 (1991).

[8] L. Knöll and D.-G. Welsch, Progr. Quant. Electron. **16**, 135 (1992).

[9] R.Y. Chiao, Phys. Rev. A **48**, R34 (1993).

[10] R.Y. Chiao, P.G. Kwiat, and A.M. Steinberg, Quantum Semiclass. Opt. **7**, 259 (1995).

[11] M. Fleischhauer and M. Schubert, J. Mod. Opt. **38**, 677 (1991).

[12] G.S. Agarwal, Phys. Rev. A **11**, 230 (1975).

[13] B. Huttner and S.M. Barnett, Europhys. Lett. **18**, 487 (1992); Phys. Rev. A **46** 4306 (1992).

[14] L. Knöll and U. Leonhardt, J. Mod. Opt. **39**, 1253 (1992).

[15] D. Kupiszewska, Phys. Rev. A **46**, 2286 (1992).

[16] S.-T. Ho and P. Kumar, J. Opt. Soc. Am. B **10**, 1620 (1993).

[17] T. Gruner and D.-G. Welsch, Phys. Rev. A **51**, 3246 (1995).

[18] S.M. Barnett, R. Matloob, and R. Loudon, J. Mod. Opt. **42**, 1165 (1995).

[19] T. Gruner and D.-G. Welsch, Preprint FSUJ TPI QO-01/95 (March, 1995); Phys. Rev. A., to be published.

[20] C.W. Gardiner and M.J. Collett, Phys. Rev. A **31**, 3761 (1985).

[21] B. Yurke, S.L. McCall, and J.R. Klauder, Phys. Rev. A **33**, 4033 (1986).

[22] R.A. Campos, B.E.A. Saleh, and M.C. Teich, Phys. Rev. A **40**, 1371 (1989).

[23] D.N. Klyshko, Phys. Lett. A **137**, 334 (1989).

[24] E. Yablonovitch and K.M. Leung, Physica **175B**, 81 (1991).

[25] A.M. Steinberg and R.Y. Chiao, Phys. Rev. A **51**, 3525 (1995).

[26] M. Born and E. Wolf, *Principles of Optics* (Pergamon Press, London, 1959).

[27] H. R. Philipp, EMIS Datareview, Aug. 1987.

[28] W. H. Louisell, *Quantum Statistical Properties of Radiation* (Wiley, New York, 1990).

[29] O. W. Greenberg, Ann. Phys. **16**, 158 (1961).

[30] P. A. Henning, Phys. Rep. **253** 5 & 6, 235 (1995).

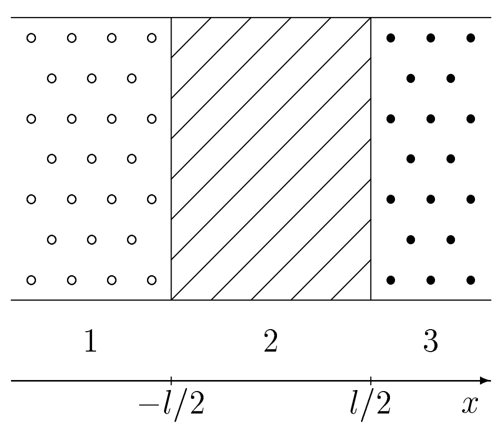

Figure 1: Scheme of the single-slab dielectric plate (2) of thickness l embedded in dielectric matter (1 and 3).

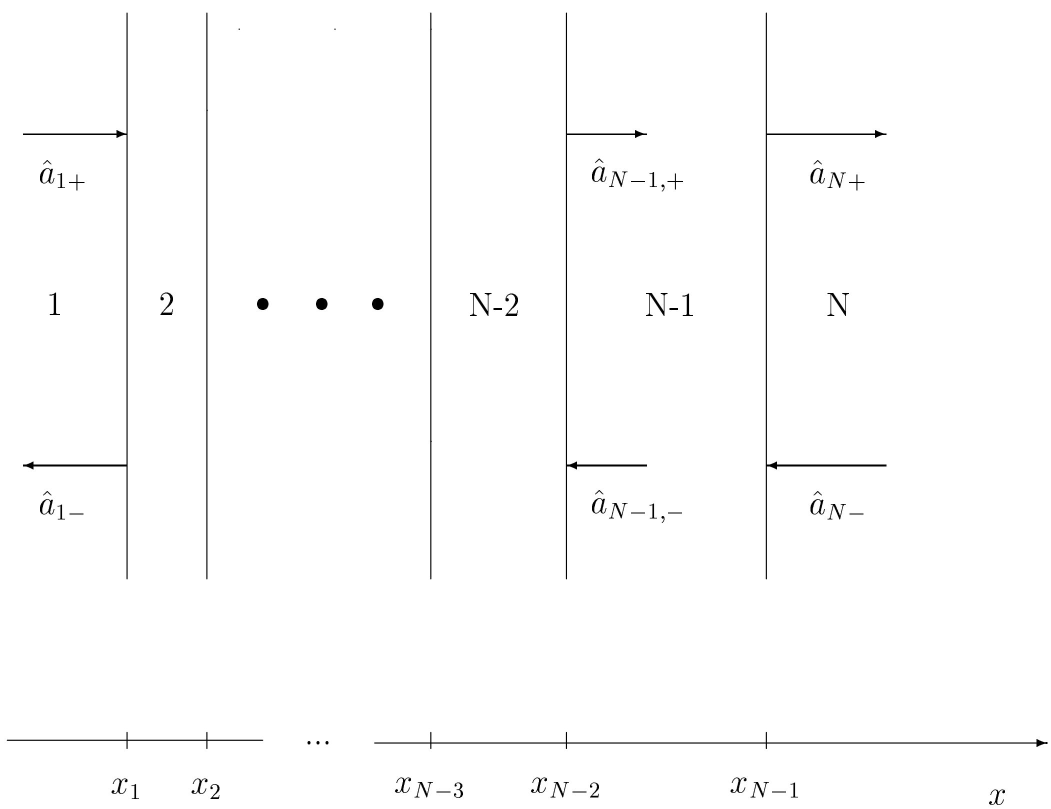

Figure 2: Scheme of the multilayer dielectric configuration, the arrows together with the amplitude operators indicating incoming and outgoing fields.

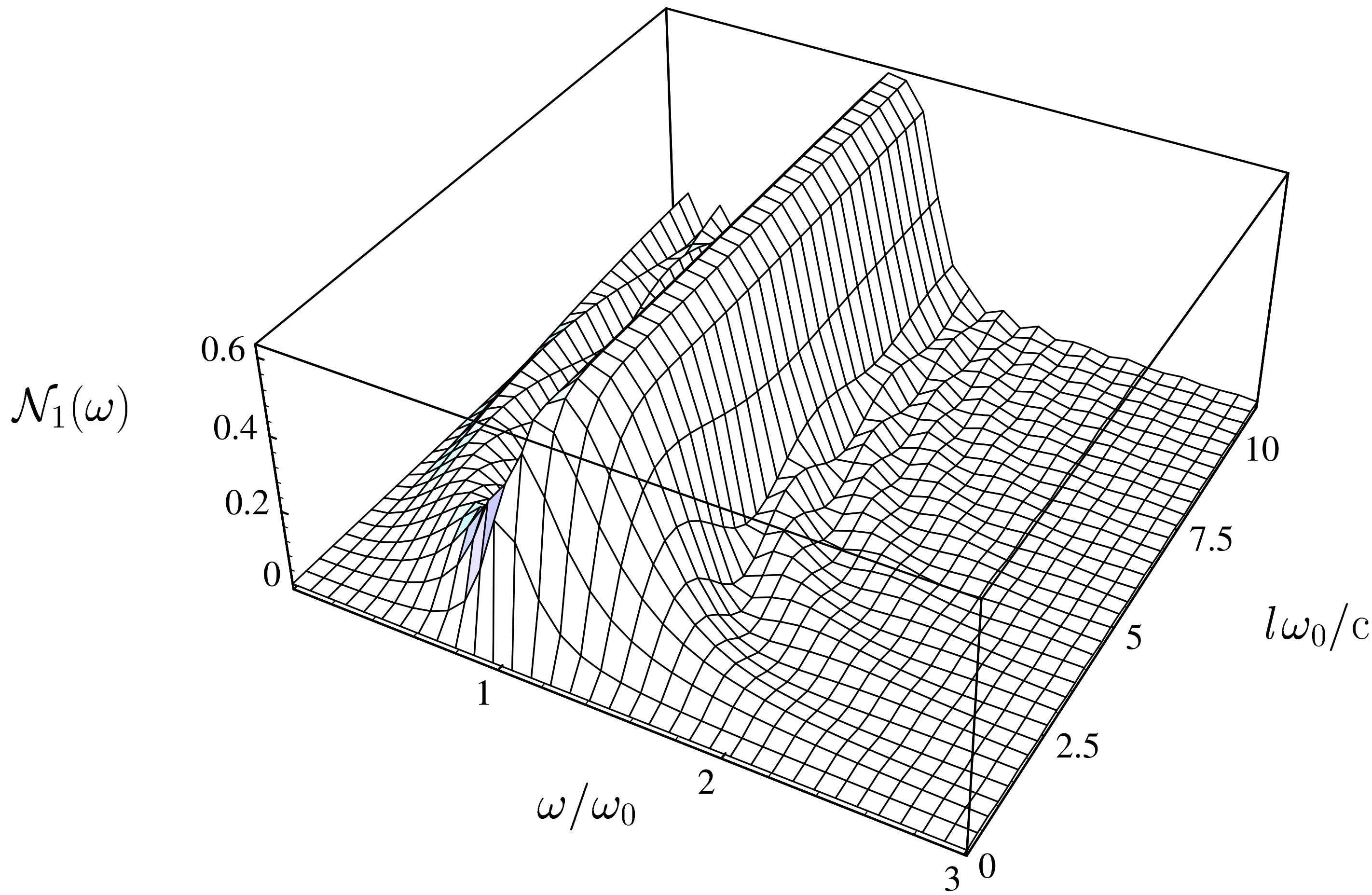

Figure 3: The ratio of photon-number densities of the reflected outgoing field and the incoming field, $\mathcal{N}_1(\omega) = N'_{\mathrm{ph}\,1}(\omega)/N_{\mathrm{ph}\,1}(\omega)$, as a function of frequency and plate thickness for a single-resonance medium ($\omega_0 = \omega_1$, $\Gamma = 0.1\omega_0$).

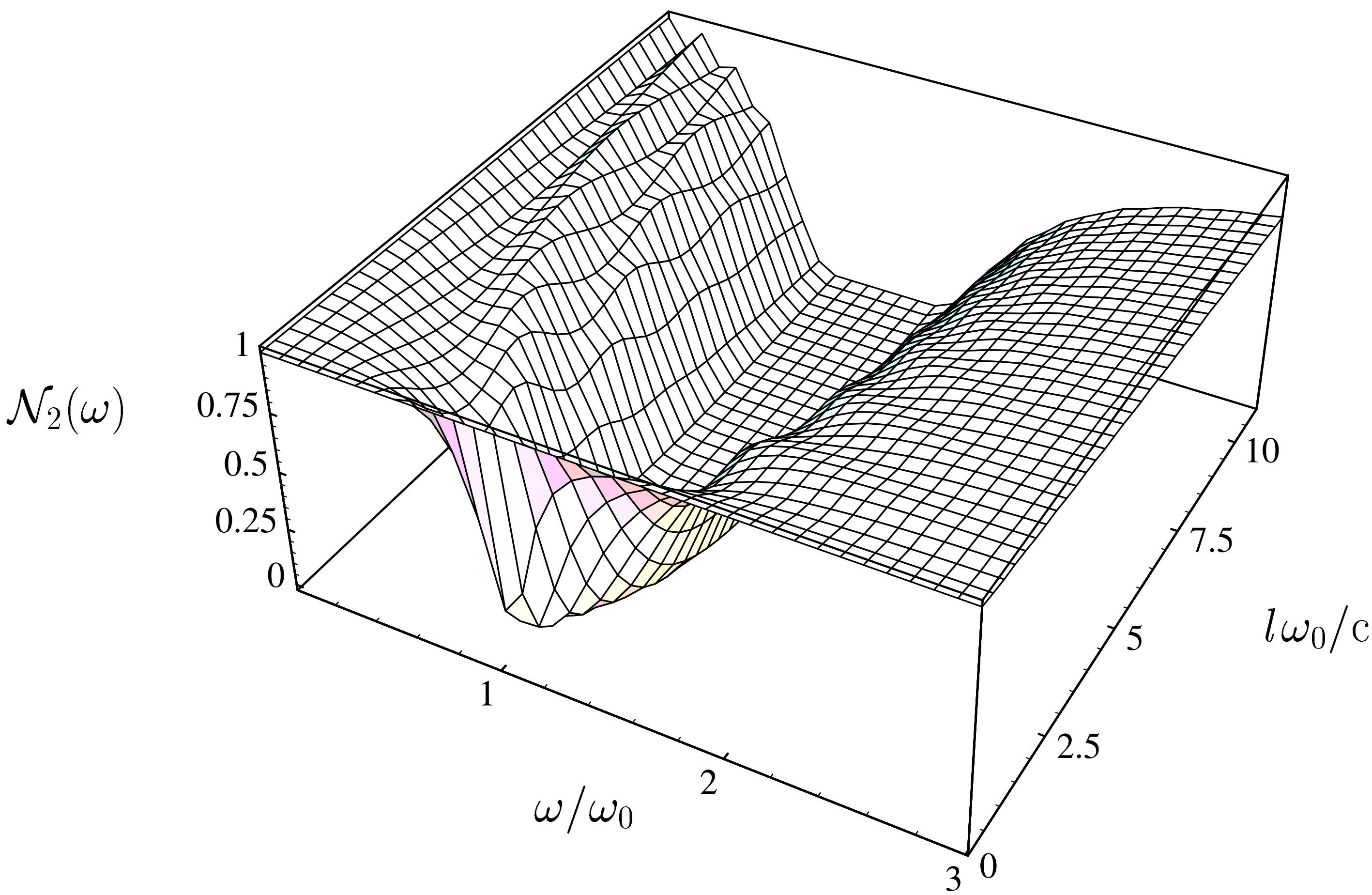

Figure 4: The ratio of the photon-number densities of the transmitted outgoing field and the incoming field, $\mathcal{N}_2(\omega) = N'_{\mathrm{ph}\,2}(\omega)/N_{\mathrm{ph}\,1}(\omega)$, as a function of frequency and plate thickness for a single-resonance medium ($\omega_0 = \omega_1$, $\Gamma = 0.1\omega_0$).

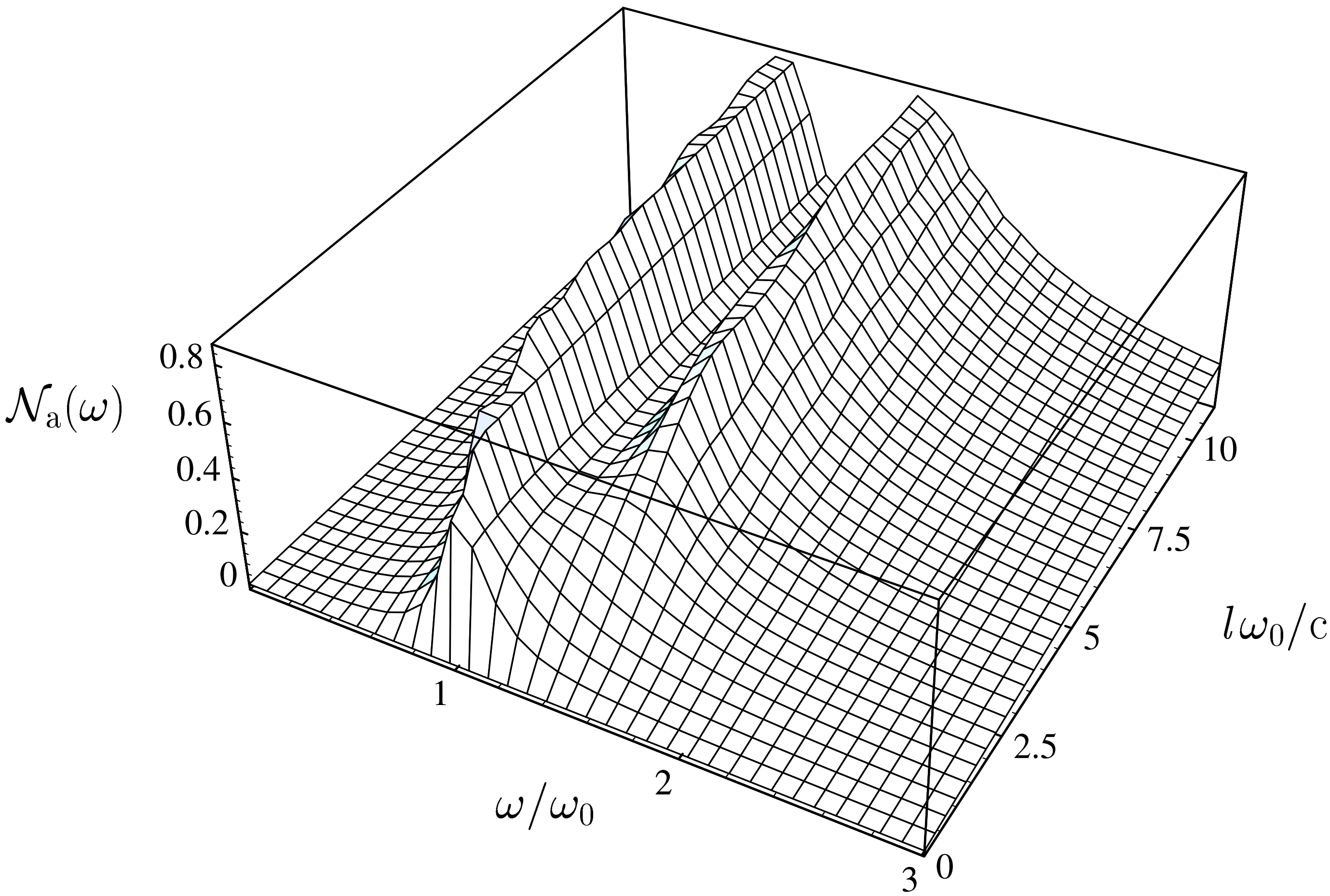

Figure 5: The ratio of the photon-number densities of the radiation absorbed in the plate and the incoming field, $\mathcal{N}_{\rm a} = [N_{\rm ph\,1}(\omega) - (N'_{\rm ph\,1}(\omega) + N'_{\rm ph\,2}(\omega))]/N_{\rm ph\,1}(\omega) = \alpha_1(\omega) = \alpha_2(\omega)$, as a function of frequency and plate thickness for a single-resonance medium ($\omega_0 = \omega_1$, $\Gamma = 0.1\omega_0$).

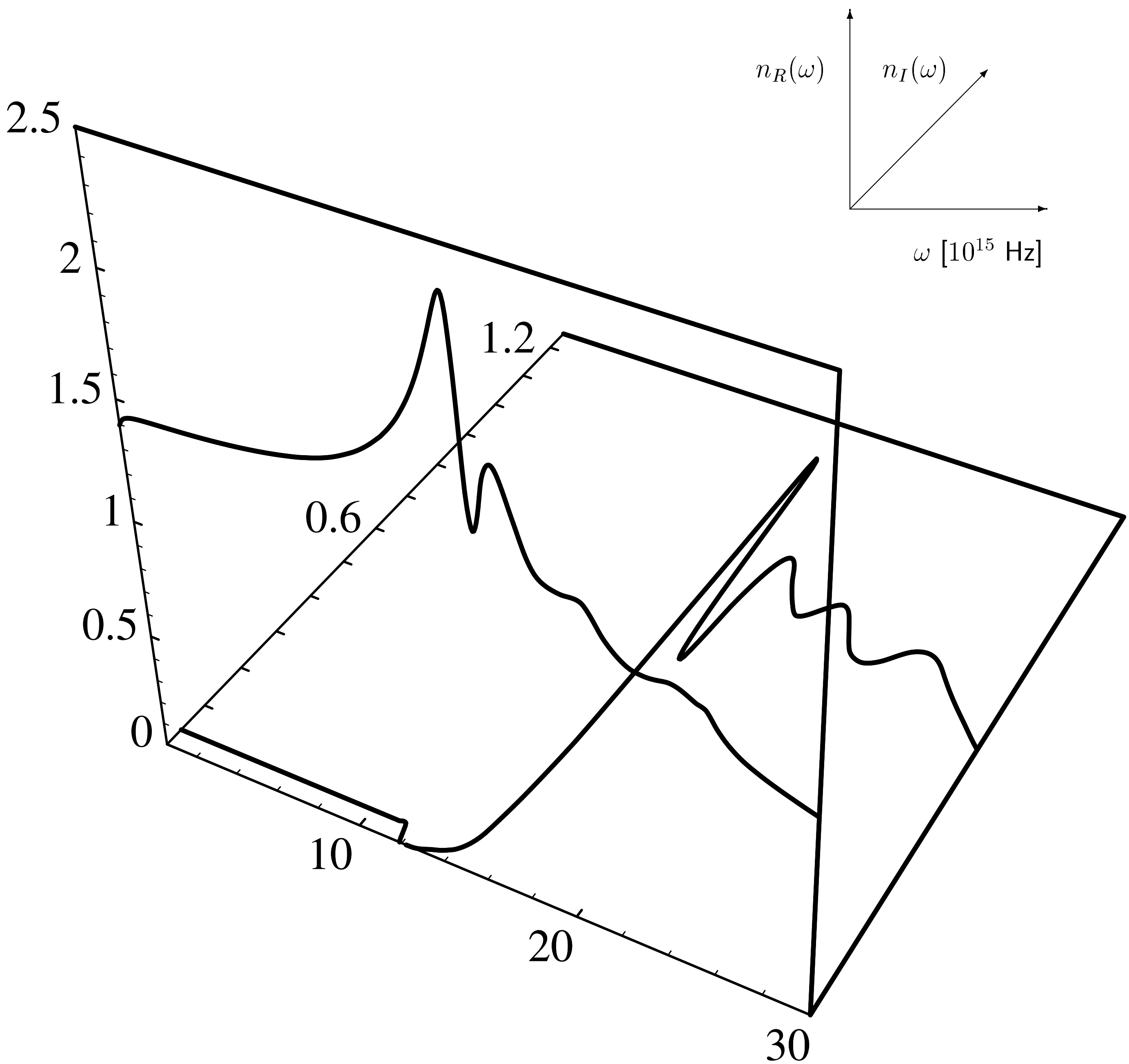

Figure 6: Real and imaginary parts of the refractive index of amorphic SiO_2 as a function of frequency.

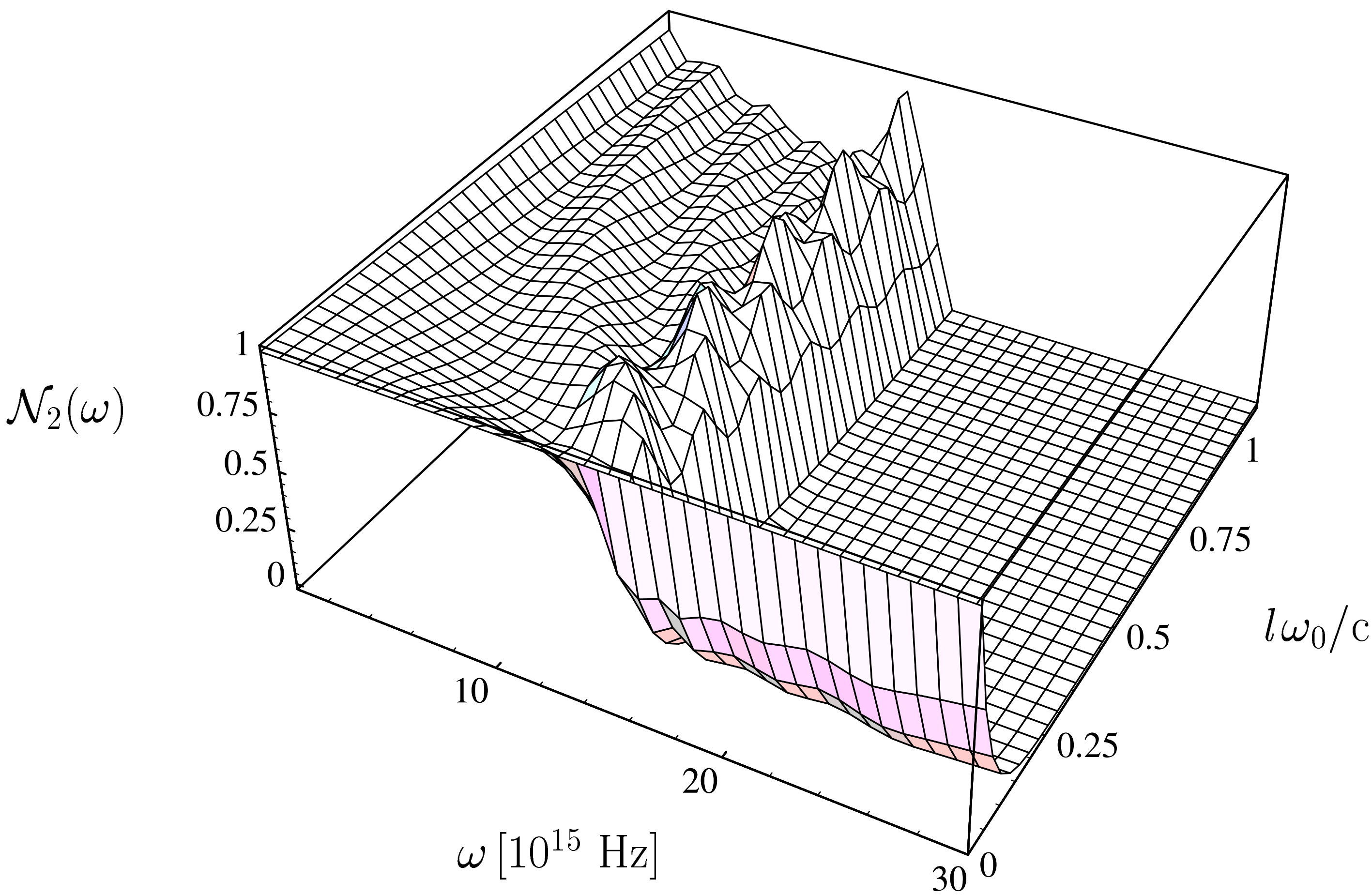

Figure 7: The ratio of the photon-number densities of the transmitted outgoing field and the incoming field, $\mathcal{N}_2(\omega) = N'_{\mathrm{ph}\,2}(\omega)/N_{\mathrm{ph}\,1}(\omega)$, as a function of frequency and plate thickness for amorphic SiO_2 ($\omega_0 = 1 \cdot 10^{15}$ Hz).